COMPLEXITY REDUCTION USING FREQUENCY MASKING TECHNIQUE FOR FIR FILTER DESIGN

By

SANJEEV KUMAR

(V00937238)

University of Visvesvaraya College of Engineering, Bangalore, India, 2013.

A Report Submitted in Partial Fulfilment of the Requirements for the Degree of

MASTER OF ENGINEERING

In the Department of Electrical and Computer Engineering

Sanjeev Kumar, 2021

University of Victoria

All rights reserved. This report may not be reproduced in whole or in part, by photocopying or other means, without the permission of the author.

COMPLEXITY REDUCTION USING FREQUENCY MASKING TECHNIQUE FOR FIR FILTER DESIGN

By

Sanjeev Kumar

University of Visvesvaraya College of Engineering, Bangalore, India, 2013.

Supervisory Committee

Dr. Panajotis Agathoklis, **Supervisor**

(Department of Electrical and Computer Engineering)

Dr. T. Ilamparithi **Departmental Member**
(Department of Electrical and Computer
Engineering)

ABSTRACT

Supervisory Committee

Dr. Panajotis Agathoklis, **Supervisor**

(Department of Electrical and Computer Engineering)

Dr. T. Ilamparithi **Departmental Member**
(Department of Electrical and Computer
Engineering)

A digital filter is an essential part of many present day electronics devices and a common type of digital filter used is Finite Impulse Response (FIR) filters. FIR filters have several advantages over Infinite Impulse Response (IIR) filters, such as easy design of linear phase FIR filters, inherently stability and low round off noise sensitivity. On the other hand, FIR filters have the disadvantage that when the design specifications require a narrow transition band, the order of FIR designs increases rapidly. One of the common techniques to design narrow transition band FIR filter is the Frequency Masking (FRM) technique which is based

on up-sampling and the use of masking filters. This leads to filters with lower order and decreased arithmetic complexity of the filter implementation.

In this project the design of linear phase FIR filters using the FRM technique is compared with some of the common ways to design linear phase FIR filters using windows. Design of linear phase low pass FIR filters using conventional window method technique is highlighted with different design examples implemented using MATLAB. The window technique has limitation as it lacks flexibility because, in design both the peak passband (δ_p) and stopband (δ_s) ripples are considered approximately equals, so that the designer can't make a passband ripple very small or a stopband attenuation very large. Further, the order of FIR filters designed using the window technique tends to increase fast when a narrow transition band is required. These design limitations can be overcome by using the frequency masking techniques which provides high selectivity with reduced arithmetic complexity. Linear phase low pass narrow bandwidth FRM FIR filter design are implemented in MATLAB and compared with the window method design in terms of filter order. Two masking filter techniques are being considered. In the first one, a masking filter technique is being used in cascade with the up-sampled model filter to design the linear phase low pass narrow transition bandwidth FIR filter. In the second, two masking filters are being used in a two channel configuration to achieve more general passbands. The comparison of these FIR filter designs indicates that the FRM technique leads to lower order FIR filters compared with the FIR filter designs using window methods at the cost of a slightly more complex design process. This reduction of filter order implies that the FRM techniques can be used to reduce arithmetic complexity for FIR filter implementations in applications requiring linear phase narrow transition bandwidth FIR filters.

Glossary

CCP – **C**onvex-**C**oncave **P**rocedure

DSP - **D**igital **S**ignal **P**rocessing

FB – **F**ilter **B**anks

FIR - **F**inite **I**mpulse **R**esponse

FRM - **F**requency **R**esponse **M**asking

IFIR – **I**nterpolated **F**inite **I**mpulse **R**esponse

IRT – **I**mpulse **R**esponse **T**runcation

LPF – **L**ow **P**ass **F**ilter

SSF – **S**ingle **S**tage **F**ilter

Table of Contents

List of Figures

List of tables

ACKNOWLEDGEMENT

Many thanks go to my supervisor, Dr. Panajotis Agathoklis for providing his support academically and personally to the successful completion of this project. I would also like to acknowledge Dr. T. Ilamparithi for serving as a supervisory committee member.

I acknowledge my family who supported me all the way with their love and words of encouragement. My dad and mom, Mr. Late Shiv Shanker and Mrs. Renu Bala Pal, you both were my backbone and rock throughout my academic journey. Thank you so much for all your prayers and encouragement.

DEDICATION

This work is dedicated to my father.

Chapter 1

Introduction

This chapter introduces digital filters and merits and demerits of FIR filters. It also provides the overview of frequency masking technique, objective and motivation for selecting this topic. Literature review provides the background in regards to frequency masking technique in filter design. At the end it gives a summary of how this project report has been organised in different chapters.

1.1 Digital filters

Electronic filters are generally assumed to be defined as continuous - time, discrete - time, or digital devices. Signals in these domains appear in one, two, or multiple dimensions. Some signals are completely parameterized by their time and/or frequency domain attributes; others are defined in some statistical sense. The function of an electronic filter is to alter or manipulate a signal's shape, energy, distributions, and other attributes in some predetermined manner. In communication applications, filters are used to detect and select signals of interest that reside within a prespecified frequency band, to suppress noise, and to correct for imperfections in a communication channel. Digital technology has ushered into existence a plethora of digital hardware, firmware, and software defined filter solutions and products [25]. In many cases, digital filters are used as an analog replacement technology. In other cases, digital technology has enabled new filters and filter applications that previously never existed [25]. Digital filters have now matured to point where they exhibit a long list of attributes including

- high precision and accuracy,
- adaptability and programmability,
- precise phase and latency control,
- robust performance over a wide range of frequencies,
- low power dissipation and low cost, and
- high reliability and repeatability [25].

1.1.1 FIR filters

These digital filters have impulse response whose duration is finite, because it settles down to zero in finite time (i.e., decays with time). The impulse response of a FIR filter with filter length N defined by the N-sample time series $h_N[\,k\,] = \{\, h[0], h\,[1], h[2]\,, h[3]\ldots., h\,[\,N-1]\}$.

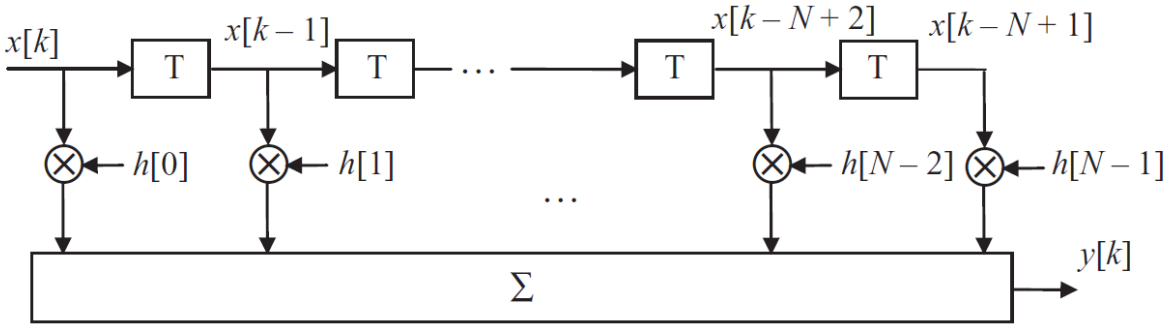

Figure 1 FIR filter consisting of shift registers, Accumulator and Multipliers with filter length N. Source [25].

Figure 1 shows direct FIR architecture, consisting a collection of shift registers configured as a first-in first-out (FIFO) array, N multipliers and an accumulator [25].

1.1.2 Advantages and disadvantages of FIR filters

FIR filter has following advantages:

- These filters can achieve linear phase response and pass a signal without phase distortion. This is to say, linear phase filters do delay the input signal but they don't distort the phase of the input signal [7].
- FIR filters are realized non recursively, hence they are inherently stable and free of limit cycle oscillation when implemented on a finite word length digital system [7].
- They are easier to implement. In effect, for most DSP microprocessors, the calculations for an FIR filter output can be done by looping a single instruction [7].

Disadvantage of FIR filters is that as the transition bandwidth becomes narrower, the filter order, and correspondingly the arithmetic complexity, increases inversely proportionally to this bandwidth [1]. As a consequence, an FIR filter of great length is required in order to approximate a frequency response with very narrow transition band.

1.2 Objective and motivation of project

In this project our focus is on reducing the computational complexity of FIR low pass filters that results when designing filters for narrow transition bandwidth. The filter order, as well as the number of nontrivial coefficients of a direct form FIR filter, is inversely proportional to the transition bandwidth. In this project we design low pass FIR filters with the traditional window method. FIR filters with small transition bandwidth suffer from high arithmetic complexity due to the high filter orders. The relation between filter length and normalised transition width has been represented in the graph below, which shows that for narrow transition width the required filter length is high, resulting in large number of computation (addition and multiplications).

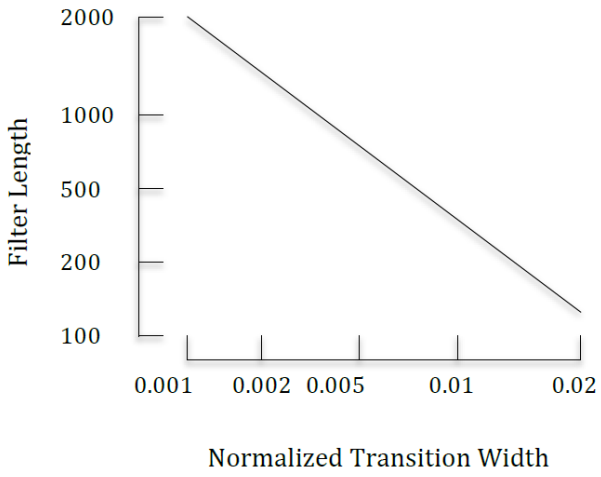

Figure 2 Filter length versus normalized transition bandwidth for an FIR low pass filter with 0.2 dB peak to peak passband ripple and -40 dB stopband ripple. Source [1]

Realization of FIR filters based on frequency response masking (FRM) has proven efficient, especially for very sharp FIR filters. An FIR is said to have sharp frequency response if its transition band(s) are extremely narrow. Designing of an FIR filter with narrow transition bands usually implies a long filter length, however the effective filter length can be considerably reduced when an FRM is employed. Lim [1] provides a plot (figure 2) of the filter length versus transition bandwidth for a minimax optimum low-pass filter with 0.2 dB peak-

to-peak passband ripple and –40dB stopband ripple. We see that the complexity becomes prohibitively high for sharp FIR filters: a normalized transition band of 0.01π, for example, requires a filter length that exceeds three hundred. To avoid this increase, the FRM approach has been proposed [1] [2]. These results have been very interesting which have been a motivating factor in order to choose this project.

1.3Frequency response masking technique

The order and complexity of the FIR filters are very high when the transition bandwidth is narrow. According to [10], for linear phase single stage filters (SSF), the filter length is roughly proportional to the inverse of the width of the transition band. A computationally efficient FIR filter design technique thus has attracted the attention of many authors in recent years [5], [11], [12],[13]. The basic idea is to compose the overall filter using several sub filters, namely, the band-edge shaping filter, its complementary, and two masking filters [15]. Filters designed using FRM technique make use of periodic sub filters as basic building block. A periodic filter has a frequency response that is periodic with a period of $2\pi/M$ rad, where M is some positive integer, as opposed to conventional digital filters for which the period is 2π rad. The band-edge shaping filter, $H_a(z^M)$, is derived by replacing each delay element of a prototype filter $H_a(z)$ by M delay elements. A drawback of linear phase FRM FIR filter is, however, that the delay is somewhat larger compared to its direct form linear-phase FIR filter counterpart.

1.4 Literature review

FRM FIR filters [4] that were proposed during 1980s with an aim to reduce the extreme computational complexity that accompanies conventional linear phase FIR filters with narrow transition band. Neuvo, Cheng-Yu and Mitra [26] proposed a particular case of filters, called interpolated FIR (IFIR) filters that can achieve very narrow transition bandwidth. However, IFIR can only be used to design FIR filters with narrow bandwidth. Lim [15] proposed a more general type of frequency response masking (FRM) structures for the design of FIR filters with small transition bandwidth and with low computational complexity. In early years, the sub filters of the FRM filters were separately designed [1], [4-5], [16-17]. As a result, the design was only sub optimal. In [18], the author proposed a two step technique for reducing the overall arithmetic complexity by simultaneously optimizing all the sub filters. First, it optimizes the masking filters by using a simple iterative design scheme. Second, the design is improved by using an efficient unconstrained nonlinear optimization algorithm [19].

The original concept of frequency response masking (FRM) was introduced by Neuvo, Cheng-Yu and Mitra [26] in 1984. It has been demonstrated that the complexity of a linear phase FIR filter can be considerably reduced by using FRM techniques. The FRM filter proposed by Neuvo, Cheng-Yu and Mitra[26] is composed of an interpolated FIR (IFIR) filter and a properly designed FIR filter. The transfer function of an IFIR filter can be obtained by replacing each unit delay z^{-1} with a delay block z^{-M}, where M is an integer. In this way, the frequency response of the IFIR filter becomes periodic over the base band with M-times narrower transition band in each frequency period. The FIR filter in the cascade is then used to mask the images from the frequency response of the IFIR filter. While this turned out to be a successful design methodology, its use is limited to the design of filters whose passband is not too wide. In 1986, Lim [1] proposed an improved approach which allows the application of FRM technique to designing a much wider range of linear phase FIR filters. It was shown that the approach given in [4] results in a linear phase FIR filter with a small fraction of nonzero coefficients, and thus is suitable for implementing sharp filters with arbitrary bandwidths. Compared to the classical single filter design, this technique offers the advantages of lower coefficient sensitivity, higher computation speed and lower power consumption.

1.5 Existing methods of FIR filter design

The commonly used methods used to design FIR filters are:

1) Impulse response truncation (windowing method)
2) Frequency sampling
3) Optimization method

Frequency sampling and optimal methods give better results for the given filter specifications, IRT (otherwise termed as windowing method) is considered as the simplest approach to design FIR filters [9]. Implementation and design of filter have been illustrated using different window functions. Design of filters have been also done using frequency marking technique which involves less computational complexity and faster processing capability.

1.6 Content and organization of report

This report has been organised in six chapters. Following paragraphs provides the glimpse of each chapter's content.

In Chapter 1 gives an overview of digital filters, objectives and motivation for this project. Discussion of FIR filters has been done along with its advantages and disadvantages. This chapter gives background of frequency masking technique and related literature.

Chapter 2 summarizes the main properties and types of FIR filters along with its design specifications needed for FIR filter design. The concept of Gibbs phenomenon has also been introduced to show the impact of truncating the impulse response in Fourier transfer domain.

Chapter 3 illustrates FIR filter design using conventional methods by the window technique. Design examples have been used to illustrated FIR filter design with given specifications. Different window functions have been used for FIR filter design illustration. This chapter discusses designing constraints and procedure used for FIR filter design using the window method. Advantages and disadvantages of window method have been discussed with respect to frequency masking technique for FIR filter design at the end of this chapter.

Chapter 4 introduces frequency masking techniques for narrow band FIR low pass filter design with one masking filter (F(z)) and its structure used for implementation. Illustration of this method has been done with a design example. Limitations of this method of design have been discussed.

Chapter 5 discusses the designing of arbitrary bandwidth FRM FIR filters. Structure and frequency response of this design involving two masking filter ($F_0(z)$ and $F_1(z)$) has been discussed. Overview of masking filters and complementary pairs has been provided. Design example has been illustrated with given specifications. At the end, the FIR filter obtained using window method and the FRM method are compared.

Chapter 6 provides future work and prospects which exist in this arena along with conclusion.

Chapter 2

Basics of FIR filter design

In this chapter, specifications and design aspects of low pass FIR filters are being discussed. It also provides the overview of different types of FIR filters. It introduces the concept of Gibbs phenomenon along with group delay and linear phase for low pass filters.

2.1 Filter specifications

Ideal Filters specifications have a zero-transition bandwidth, a constant passband, and a stopband with an infinite attenuation. In actual practical design it is very difficult to achieve these specifications and hence, some amount of tolerance is allowed. The permissible tolerances should be specified before designing the filter. For an LPF, we often have the following frequency response specifications:

δ_p: Peak passband deviation

δ_s: Stopband deviation

ω_p: Passband cut-off frequency

ω_s: Stopband cut-off frequency

N: Filter length (N=P+1)

P: Order of the FIR

$\Delta\omega$: Transition bandwidth

T: Sampling period

$\Omega = \omega.\frac{1}{f_c} = 2\pi\left(\frac{f}{f_c}\right)$, {where $\frac{f}{f_c}$ is normalised frequency}

All these specifications are depicted in figure 4. In general, δ_p and δ_s on a linear scale are very small and it is often convenient to express them in dB. Therefore, attenuation factors expressed in terms of A_p and A_s (defined in equation 2.1 and 2.6) respectively [9]

Passband attenuation A_p:

$$A_p = 20 \log_{10} \left(\frac{1+\delta p}{1-\delta p}\right) \quad (2.1)$$

And Stopband attenuation A_s is explained below:

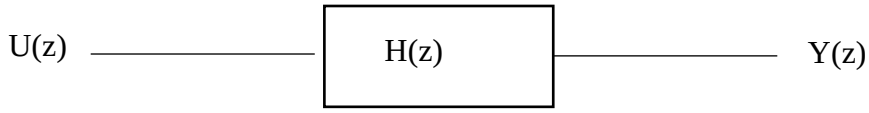

Figure 3 Transfer function. Source [28]

From figure 3, transfer function H(z) is given by [28]

$$H(z) = \frac{Y(z)}{U(z)} = \left(\frac{N(z)}{D(z)}\right) \quad (2.2)$$

Attenuation, A(ω) is given by

$$A(\omega) = 20 \log_{10} \left(\frac{1}{H(e^{j\omega})}\right) = -20 \log_{10} \left(H(e^{j\omega})\right) \quad (2.3)$$

Minimum Stopband Attenuation:

$$A_s = \min_{\omega} (A(\omega)) \text{ for } \omega \in \text{stopband} \quad (2.4)$$

$$A_s = \min_{\omega} (-20 \log (H(e^{j\omega})) \quad (2.5)$$

$$A_s = \max_{\omega} (20 \log (H(e^{j\omega})) , \omega \in \text{stopband} \quad (2.6)$$

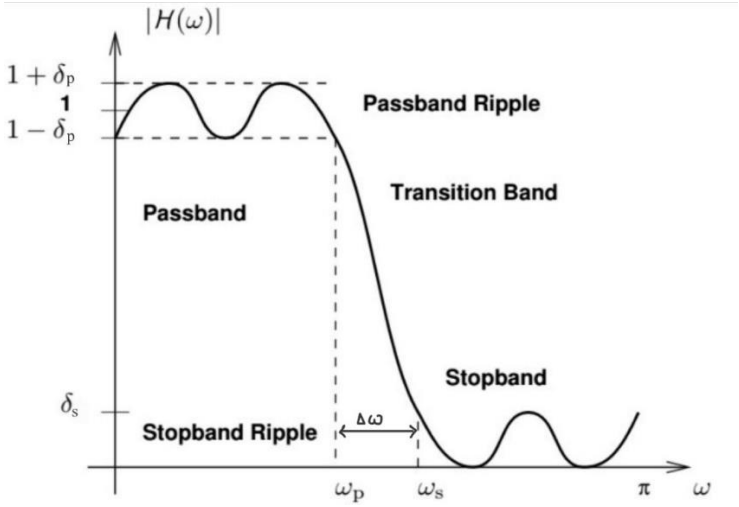

Figure 4 Filter specifications. Source [27]

2.2 Types of FIR filter

Depending on the value of the filter length N and the nature of the impulse response whether symmetric or asymmetric, four types of linear phase FIR digital filters can be defined [7].

Type I FIR filter: If the filter order P is even (or the filter length N = P+1 is odd) and the impulse response is symmetric, then the FIR filter is termed type I linear phase FIR filter. In this case, we can express the impulse response sequence as

$$h[n] = h[P-n], 0 \le n \le P, \tag{2.7}$$

and its frequency response is found to be

$$H\left(e^{j\Omega}\right) = \sum_{n=0}^{P} h[n]e^{-jn\Omega} = \sum_{n=0}^{\frac{P}{2}-1} h[n]\left\{e^{-jn\Omega} + e^{-j(P-n)\Omega}\right\} + h\left[\frac{P}{2}\right] e^{-j\frac{P}{2}\Omega} \tag{2.8}$$

After simplification of (2.8), frequency response of type I FIR filter is obtained as

$$H\left(e^{j\Omega}\right) = e^{-j\frac{P}{2}\Omega}\left\{h\left[\frac{P}{2}\right] + 2\sum_{n=1}^{\frac{P}{2}} h\left[\frac{P}{2}-n\right]\cos(n\Omega)\right\} = e^{-j\frac{P}{2}\Omega}\hat{H}\left(e^{j\Omega}\right), \tag{2.9}$$

where $\hat{H}\left(e^{j\Omega}\right)$ is a real function of Ω. From equation (2.9), it can be observed that the phase response of type I FIR filter is linear with a delay of P/2 samples [7].

Type II FIR filter: An FIR filter is said to be type II if its degree or order P is odd and its impulse response sequence is symmetric, as defined in (2.7). Using equation (2.7) in (2.8), frequency response of type II FIR filter after simplification can be expressed as

$$H(e^{j\Omega}) = e^{-j\frac{P}{2}\Omega}\left\{2\sum_{n=1}^{\frac{P+1}{2}} h\left[\frac{P+1}{2}-n\right]\cos\left(\left(n-\frac{1}{2}\right)\Omega\right)\right\} \quad (2.10)$$

It can be seen that quantity within the braces is real and the phase response is linear with delay of $\frac{P}{2}$ samples [7].

Type III FIR filter: In this case the filter order or degree is even and the impulse response is asymmetric as defined by

$$h[n] = -h[P-n], 0 \le n \le P \quad (2.11)$$

The frequency response of type III FIR filter can be shown to be

$$H(e^{j\Omega}) = je^{-j\frac{P}{2}\Omega}\left\{2\sum_{n=1}^{\frac{P}{2}} h\left[\frac{P}{2}-n\right]\sin(n\Omega)\right\} \quad (2.12)$$

The quantity within the braces in (2.12) is real and the phase response is linear with a delay of $\frac{P}{2}$ samples [7].

Type IV FIR filter: The type IV FIR filter has an odd degree and its impulse response is asymmetric as defined in (2.11). Using these facts, we can express its frequency response as

$$H(e^{j\Omega}) = je^{-j\frac{P}{2}\Omega}\left\{2\sum_{n=1}^{\frac{P+1}{2}} h\left[\frac{P+1}{2}-n\right]\sin\left(\left(n-\frac{1}{2}\right)\Omega\right)\right\} \quad (2.13)$$

It can be seen from (2.13), the quantity within the braces is real and so the phase response is linear with a delay of $\frac{P}{2}$ samples [7].

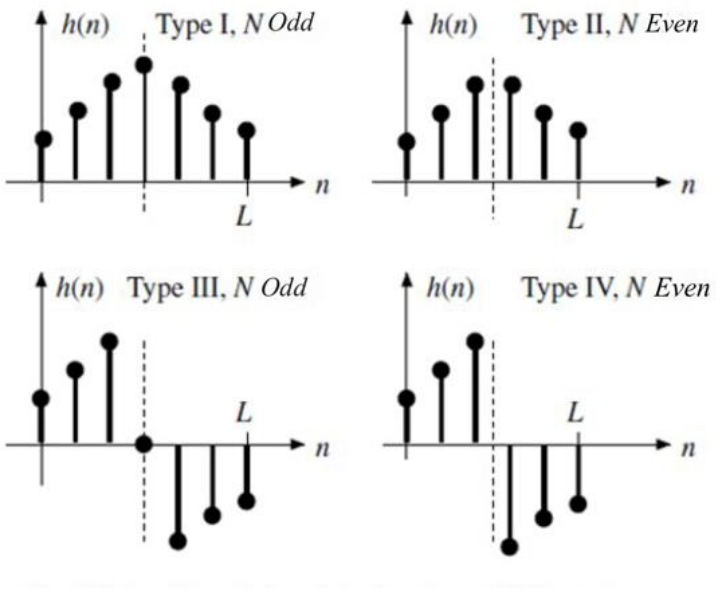

Figure 5 Typical impulse response for the four types of linear phase FIR filters. Source [15].

2.3 Linear phase low pass filter

Frequency response of an ideal LPF with linear phase can be defined as [22]

$$H_{lp}(e^{j\omega}) = \begin{cases} e^{-j\omega\alpha} , & |\omega| \leq \omega_c \\ 0, & \omega_c < |\omega| \leq \pi. \end{cases} \quad (2.14)$$

While magnitude response of ideal low pass filter is [22]

$$|H_{lp}(e^{j\omega})| = \begin{cases} 1 , & |\omega| \leq \omega_c \\ 0, & \omega_c < |\omega| \leq \pi. \end{cases} \quad (2.15)$$

And the phase response is

$$\text{Arg } H_{lp}(e^{j\omega}) = -\alpha\omega. \quad (2.16)$$

Group delay ($d_g(\omega)$) (defined in 2.17) is one of the parameters used to measure the linearity of the phase. In some literature group delay is defined as the time delay of the amplitude envelops of the various sinusoidal components of a signal through the device under test, and is a function of frequency for each component. The delay variation means that signals consisting of multiple frequency components will suffer distortion because these components are not delayed by the same amount of time at the output of the device. This changes the shape of the signal in addition to any constant delay or scale change. A sufficiently large delay variation can cause problems such as poor fidelity in audio or inter symbol interference (ISI).[24]

Group delay is defined as

$$d_g(\omega) = -\frac{d}{d(\omega)} (\text{Arg } H(e^{j\omega})) \quad (2.17)$$

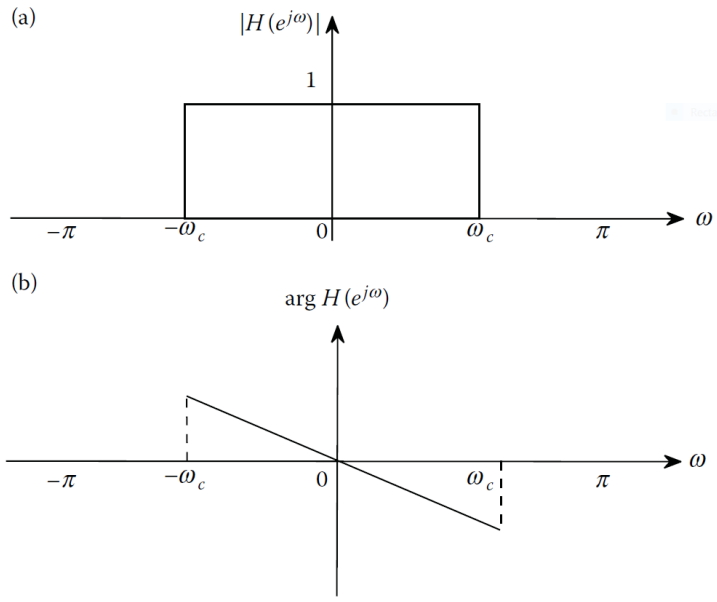

Figure 6 Ideal LPF with linear phase: a) Magnitude response and b) Phase response.

The magnitude response and the phase response of the ideal LPF, with linear phase, are shown in figure 6. Group delay for linear phase filters is nothing but the point of symmetry of impulse response. Although there is no phase (or delay) distortion in either zero delay or constant group delay for ideal filters, these filters are non-realizable due to their infinite extent. The number of coefficients that should be considered to design a causal filter depends on the specifications. Once the filter length is calculated, we can find the value of α (group delay) using the relation

$$\alpha = \frac{N-1}{2} \quad (2.18)$$

The coefficients of the FIR filter are therefore given by

$$h[n] = h_d[n]\, f[n] \quad (2.19)$$

where f [n] represents the samples of the discrete-time data window that extends from 0 to $N - 1$ and $h_d[n]$ represents the ideal infinite time impulse response obtained as the inverse Fourier transform of the $H(e^{j\omega})$ desired impulse response and h[n] is the FIR impulse response.

2.4 Gibbs phenomenon

In order to obtain the frequency response of the FIR filter, the desired frequency response $H_d(e^{j\omega})$ is convolved with the frequency response of the window $F(e^{j\omega})$ (shown in figure 7). The resulting response $H(e^{j\omega})$ is depicted in figure 7(c). For illustration purpose a rectangular window has been considered.

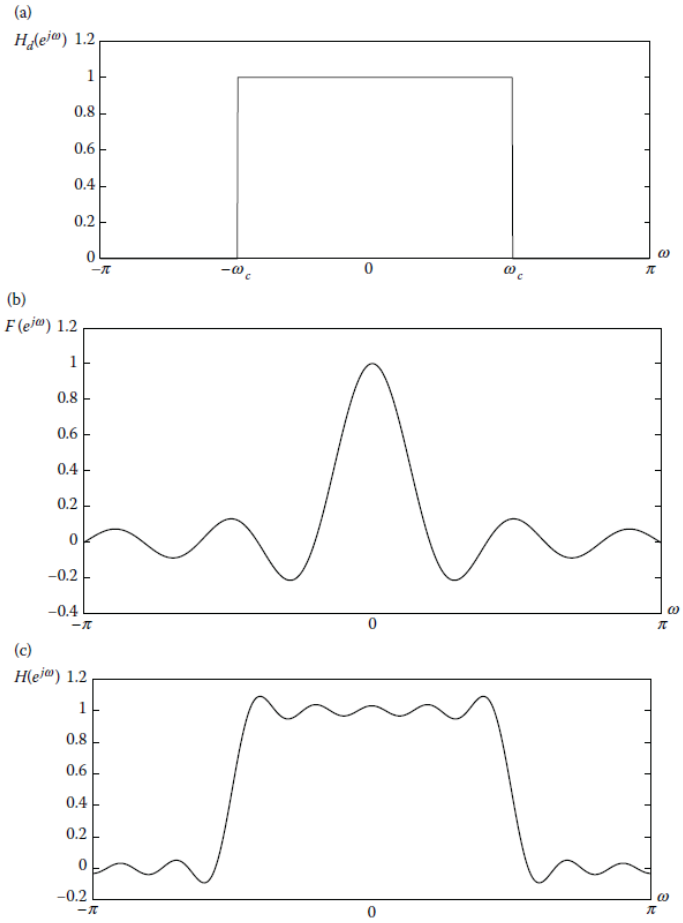

Figure 7 Truncation of impulse response using the rectangular window.

a) Desired frequency response. (b) Frequency response of a rectangular window. (c) Frequency response of FIR impulse response.

It can be observed that $F(e^{j\omega})$ figure 7(b) has the main lobes and side lobes. The side lobes present in the Fourier transform of the window are responsible for the ripples in the stopband and passband of $H(e^{j\omega})$, whereas the main-lobe width of the Fourier transform of the window is responsible for the nonzero transition width of $H(e^{j\omega})$, figure 7(c). To obtain a narrow transition band, increase in the value of N (i.e., number of coefficients in the filter response) is required. However, higher values of N require more computations. Therefore, trade-off between smearing of the desired response and the computational complexity exits. This

minimum attenuation is termed as *Gibbs number* [9]. Gibbs number for the rectangular window is 0.0895[9]. This is illustrated in figure 8 where transition bandwidth of the filter designed with N= 101 has a steeper transition band than the one designed with N= 21. Although a rectangular window gives the smallest transition width for a given value of N, its side lobes are much larger. By tapering the window at both ends, we can reduce the side lobe levels, but at the expense of increased main lobe widths, thereby increasing the transition bandwidth [9].

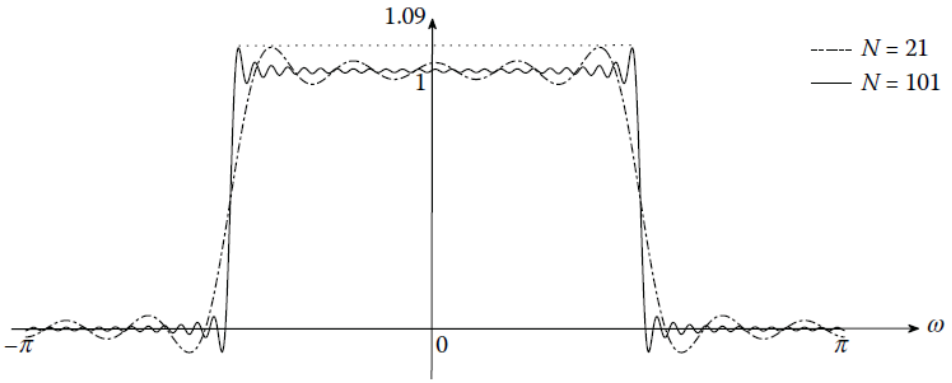

Figure 8 FIR filter designed with direct truncation with filter lengths N= 21 and N = 101. Source [9]

2.5 Summary

Different types of FIR filters were discussed in detail and low pass filter design specifications were introduced. The concept of Gibbs phenomenon was introduced, illustrating the impact of truncating the impulse response in Fourier transfer domain.

Chapter 3

FIR Filter design using windows

This chapter discusses designing of FIR filters using one of the most commonly used techniques known as window method. Low pass FIR filter design methods and constraints are been discussed in detail. Design of low pass FIR filters is illustrated using different windows for given specification examples.

3.1 Designing constraints

Based on the design specifications a possible FIR filter design technique is the impulse response truncation (IRT). FIR filter design using windows is easier and simpler to design with less complications.

Filters designed by the windowing method exhibit the following properties:

- The frequency response near a discontinuity of the ideal filter is approximately antisymmetric about a point of discontinuity in the neighbourhood of that discontinuity.
- The width of the transition band is inversely proportional to the length of the window.

Thus, to achieve a prescribed stopband attenuation and passband ripple, the designer must choose a suitable window and the length of the window to achieve the required transition band. Advantage of window method over frequency masking technique is that it is easier and simpler to design with less complications.

3.2 Design procedure for filters using window technique

Given the specification parameters, passband frequency(ω_p), stopband frequency (ω_s), passband ripple (δ_p) and stopband ripple (δ_s)

1. First, we design an ideal filter with the given specifications, by assuming the cut-off frequency (ω_c) to be the mean of passband and stopband cut-off frequencies, that is,

$$\omega_c = \frac{\omega p + \omega s}{2} .$$

2. Impulse response $h_d[n]$ of the ideal filter is determined using inverse Fourier transform, in our analysis we used low pass filter design as explained in section 2.3.
3. Transition bandwidth of filter is dependent on main lobe width of window. Selection of window is done so that it has the required main lobe width which can satisfy the transition bandwidth requirement. Various windows with their characteristic have been tabulated in table 1.
4. Find the number of filter coefficients (N) using the relation between transition bandwidth and N given in table 1.
5. Truncate the impulse response using the selected window to obtain the symmetric filter coefficients.
6. Value N computed in step 4 is only an approximate value. Therefore, if the desired filter specifications are not met, then repeat the procedure with a different value of N [9].

Filter Characteristics Using Different Windows

Window	Peak Side-Lobe Level [dB]	Transition Width
Rectangular	−13	$4\pi/N$
Bartlett	−26	$8\pi/N$
Riesz	−21	$5.72\pi/N$
Riemann	−27	$6.56\pi/N$
Hann	−31	$8\pi/N$
Bohman	−46	$12\pi/N$
Hamming	−41	$8\pi/N$
de la Vallé-Poussin	−53	$16\pi/N$
Blackman	−57	$12\pi/N$

Table 1 Characteristics of different windows. Source [9]

3.3 FIR filter design example using window technique

Design example 3.1: Design low pass filter with cut off frequency = 0.4π and N=20 using window technique.

In this example we will illustrate the properties of the various windows using the low pass filter explained in section 2.3.

3.3.1 Rectangular window

Rectangular window (also known as Boxcar window) is defined

$$w[n] = \begin{cases} 1, & 0 \le n \le N \\ 0, & \text{otherwise} \end{cases} \qquad (3.1)$$

Figure 9 shows the plot of rectangular window for design example 3.1. Discrete time Fourier transform of rectangular window is given by [22]

$$W(e^{j\omega T}) = \frac{\sin\left(\frac{[N+1]\omega T}{2}\right)}{\sin\left(\frac{\omega T}{2}\right)} e^{-\frac{jN\omega T}{2}} \qquad (3.2)$$

$W(e^{j\omega T})$ is shown in figure 10 ,convolved with the ideal frequency response $H_i(e^{j\omega T})$, and the resulting frequency response $H(e^{j\omega T})$ exhibits Gibbs oscillations at a discontinuity in the ideal frequency response seen in figure 11.

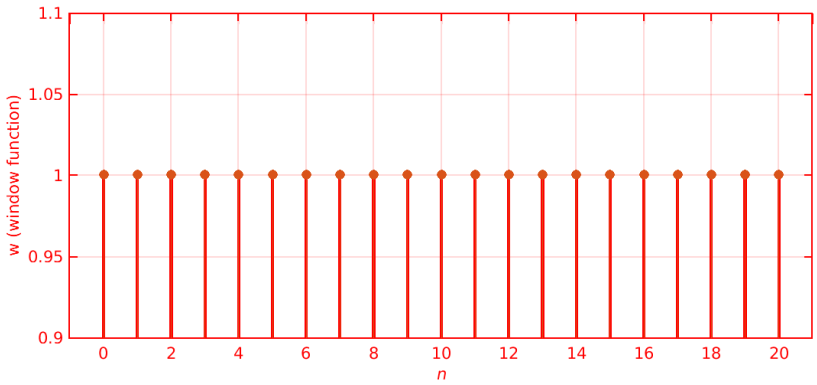

Figure 9 Rectangular window function sequence for filter design with N=20.

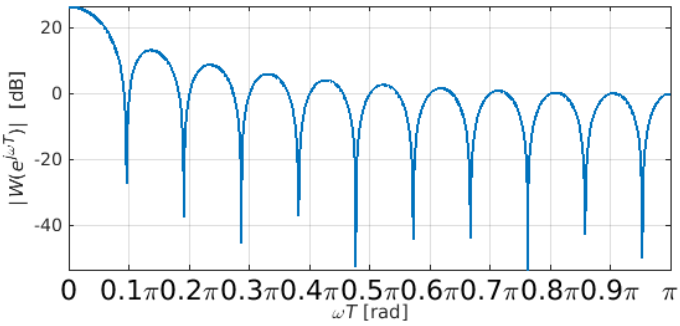

Figure 10 Magnitude responses of a rectangular window.

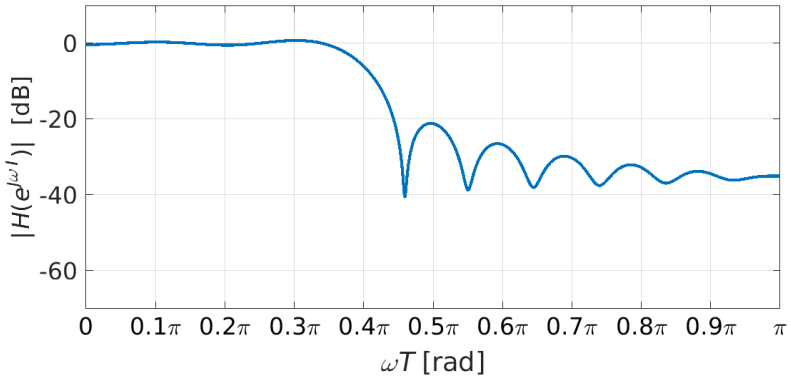

Figure 11 Magnitude responses of a linear phase FIR designed using rectangular window for design example 3.1

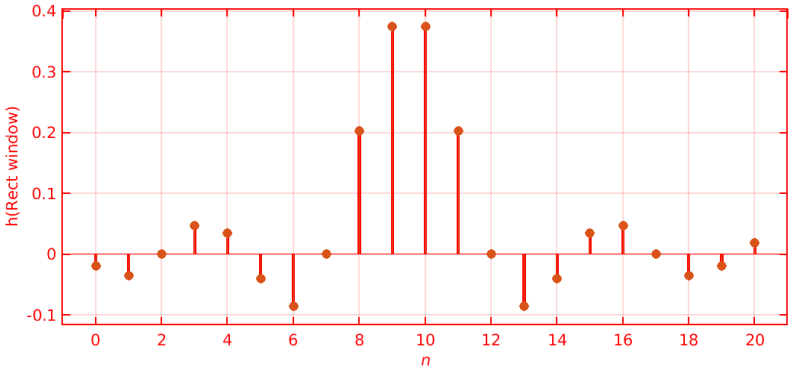

Figure 12 Impulse response of low pass filter designed using rectangular window

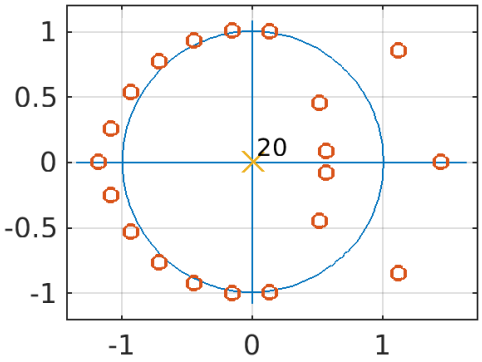

Figure 13 Pole-zero configuration for the linear phase FIR filter designed with a rectangular window and N = 20

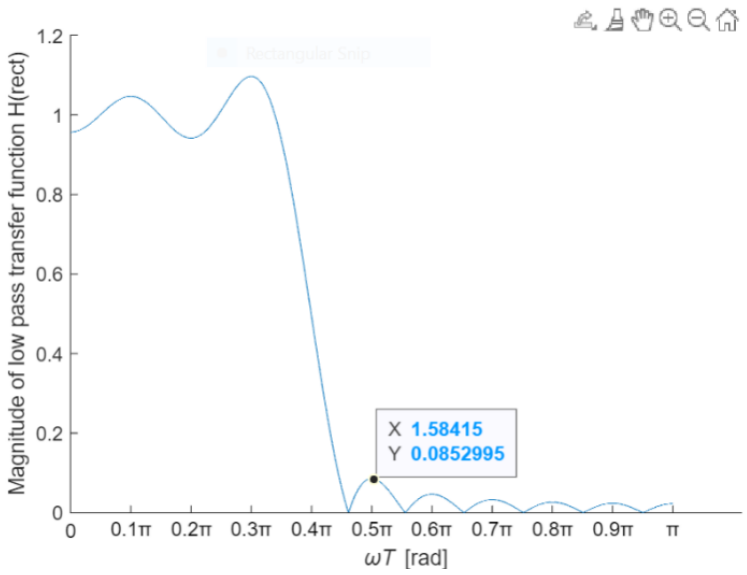

Figure 14 Stopband attenuation factor A_S

Figure 13 shows the pole-zero configuration for the linear phase FIR filter. It can be observed from the figure that the majority of the zeros lie on the unit circle where they generate the stopband attenuation and zeros in the passband region are mirrored in the unit circle. All poles lie at the origin. Figure 14 shows minimum stopband attenuation factor (A_s).

3.3.2 Von Hann (Hanning) window

The von Hann window, which is also known as the Hanning window, was proposed by the Austrian metrologist Julius Von Hann (1839–1921), is defined by [22]

$$w[n] = \begin{cases} \frac{1}{2}\left(1 + \cos\left(\frac{2n\pi}{N+1}\right)\right), 0 \leq n \leq N \\ 0, \text{otherwise} \end{cases} \quad (3.3)$$

Changing the window function may reduce the size of the Gibbs' oscillations and produce a frequency response with smaller errors in the passbands and stopbands, at the expense of widening of the transition band at the discontinuity [22].

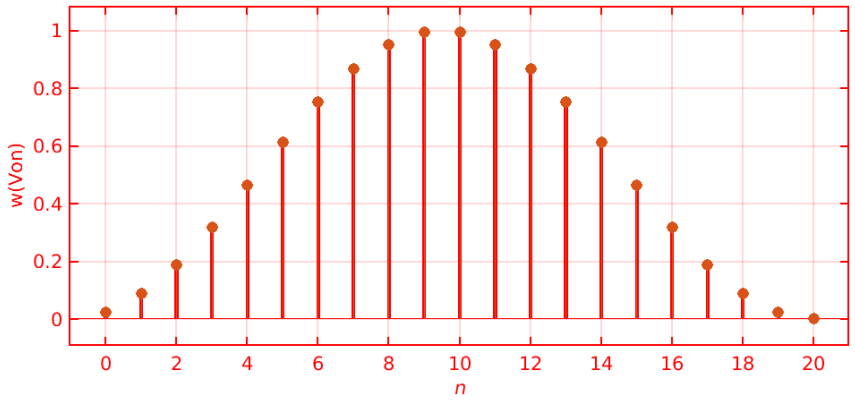

Figure 15 Von Hann window function sequence for filter design with N=20.

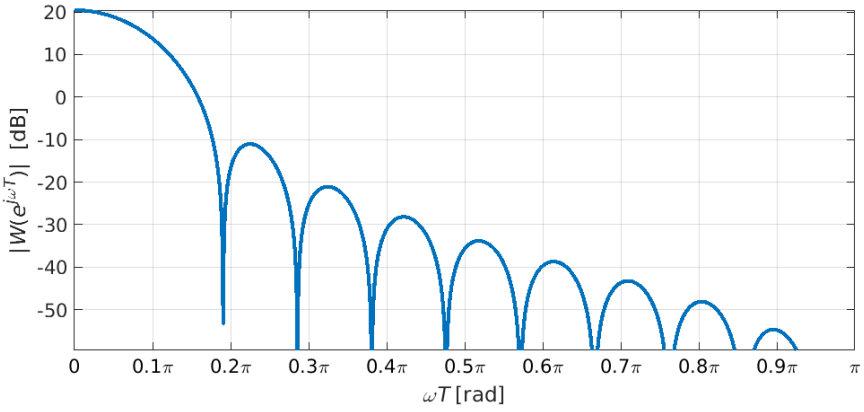

Figure 16 Magnitude responses of Von Hann window

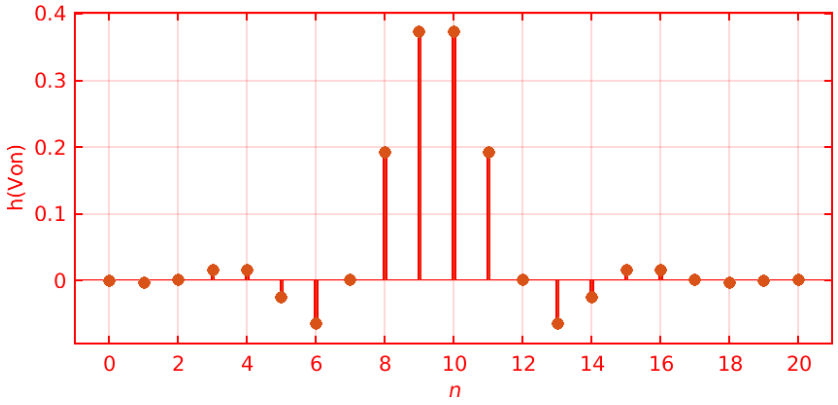

Figure 17 Impulse response of low pass filter designed using Von Hann window

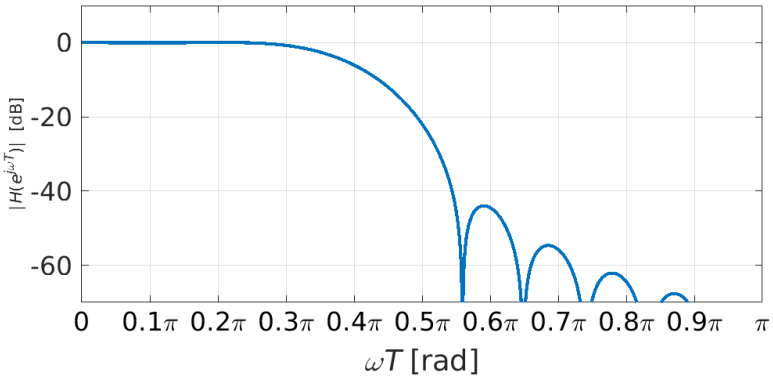

Figure 18 Magnitude responses of a linear phase FIR designed using Von Hann window for design example 3.1

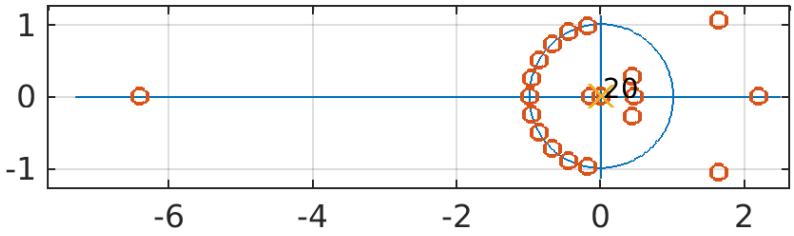

Figure 19 Pole-zero configuration for the linear phase FIR filter designed with a Von Hann and N = 20

It can be remarked that the filter magnitude becomes smaller for higher frequencies. Figure 19 shows the pole-zero configuration.

3.3.3 Hamming window

The Hamming window is defined as [22]

$$w[n] = \begin{cases} 0.54 + 0.46\,cos\left(\frac{2(n-1)\pi}{N}\right), 0 \le n \le N \\ 0, otherwise \end{cases} \quad (3.4)$$

Figure 20 shows the function sequence for design example 3.1. Magnitude response of window is shown in figure 21.

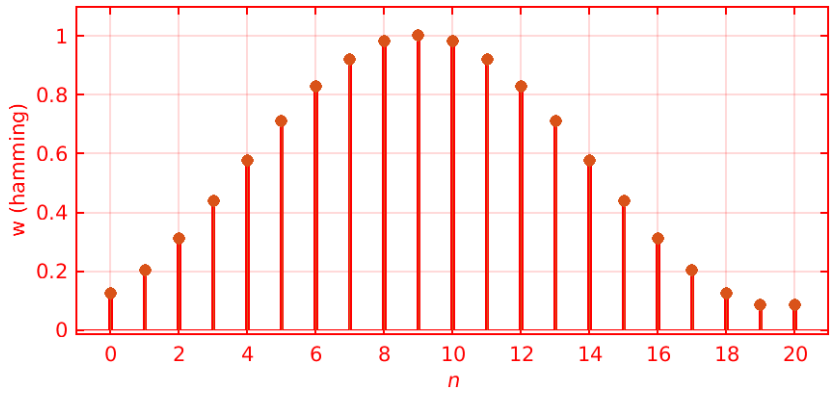

Figure 20 Hamming window function sequence for filter design with N=20.

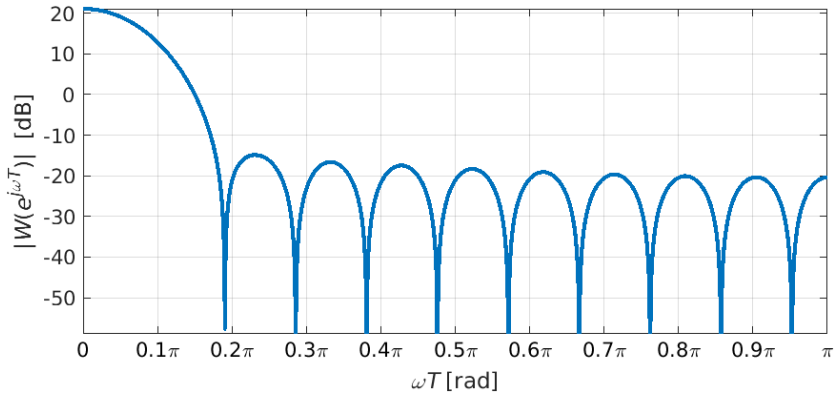

Figure 21 Magnitude responses of Hamming window

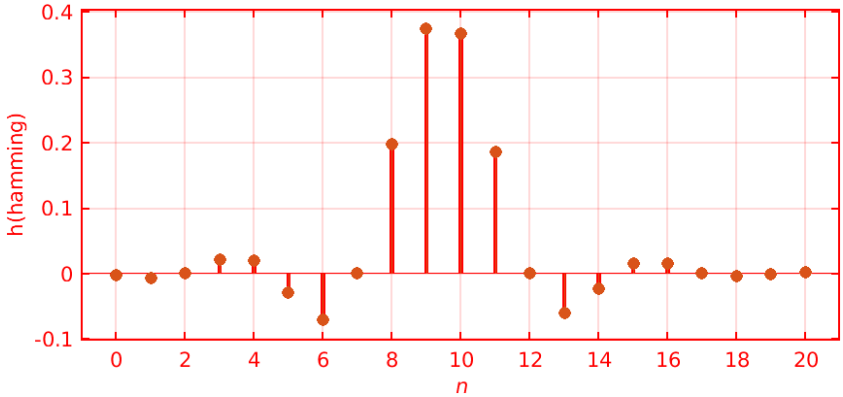

Figure 22 Impulse response of low pass filter designed using Hamming window

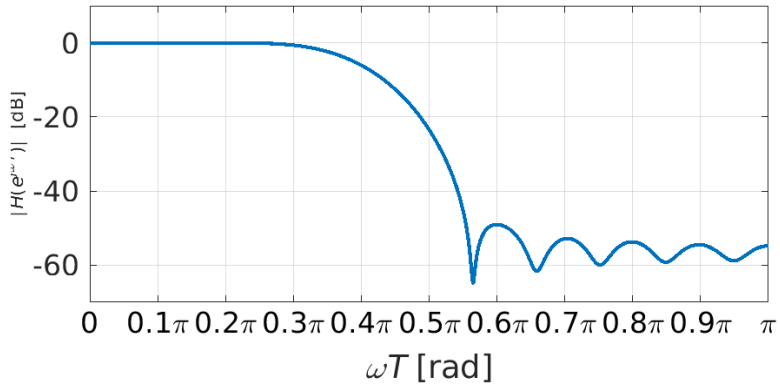

Figure 23 Magnitude responses of a linear phase FIR designed using Hamming window for design example 3.1

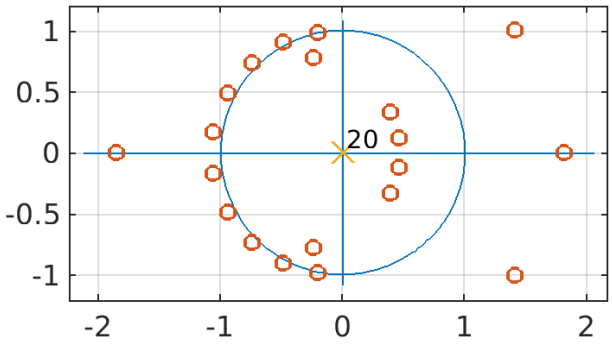

Figure 24 Pole-zero configuration for the linear phase FIR filter designed with Hamming window and N = 20

3.3.4 Bartlett window

The Bartlett window is defined as [22]

$$w[n] = \begin{cases} \left(\frac{2(n+0.5)}{N+1}\right), 0 \le n \le N/2 \\ (2 - \frac{2(n+1.5)}{N+1}, \frac{N+1}{2} \le n \le N \\ 0, \text{otherwise} \end{cases} \quad (3.5)$$

As can be seen from (3.5), Bartlett's window tapers off linearly. Magnitude responses for the window and a linear-phase lowpass FIR filter designed using this window function is shown in figure 26 and figure 28 respectively.

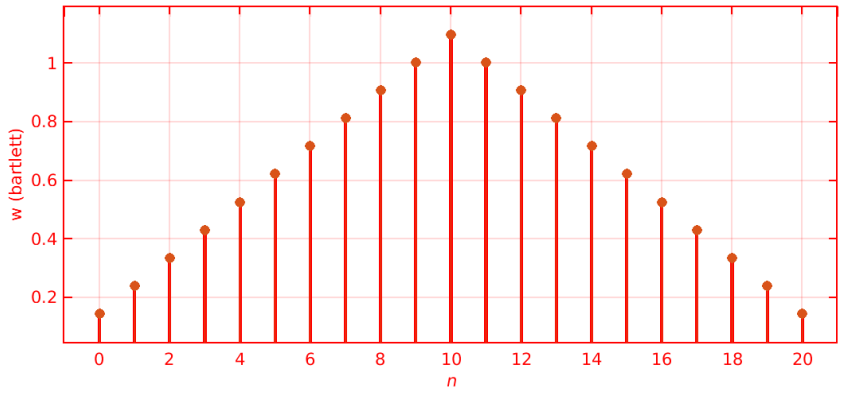

Figure 25 Bartlett window function sequence for filter design with N=20.

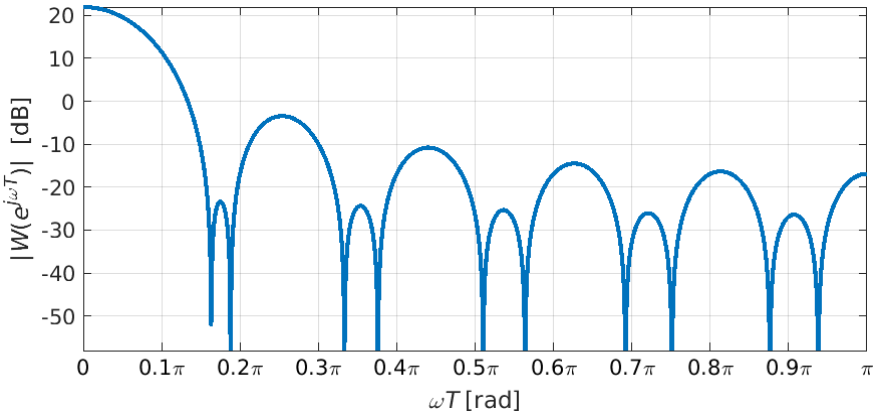

Figure 26 Magnitude responses of a Bartlett window

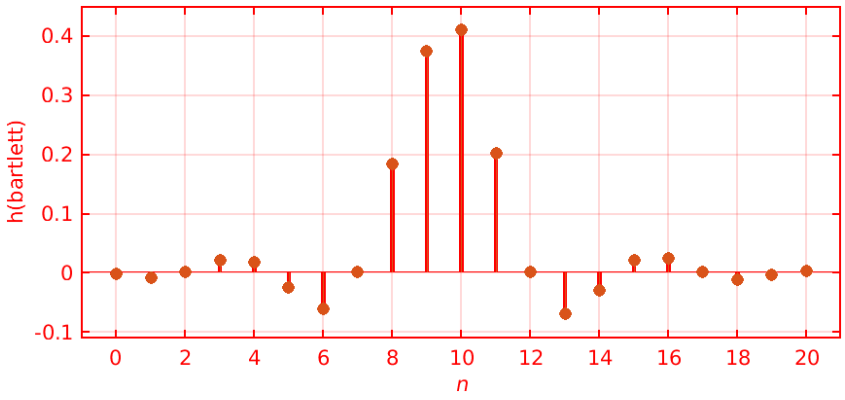

Figure 27 Impulse response of low pass filter designed using Bartlett window

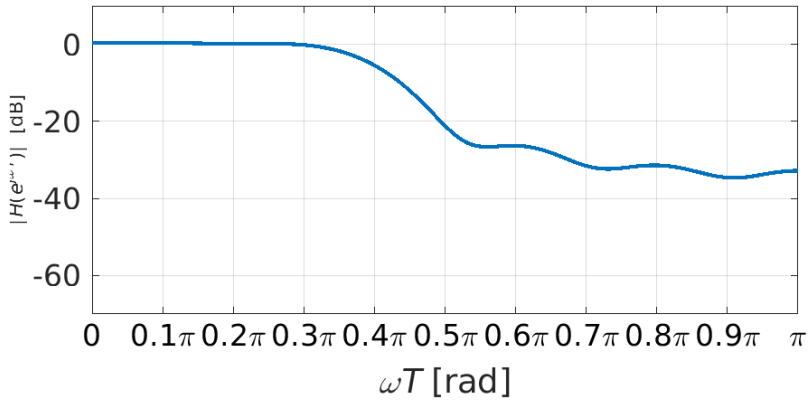

Figure 28 Magnitude responses of a linear phase FIR designed using Bartlett window for design example 3.1

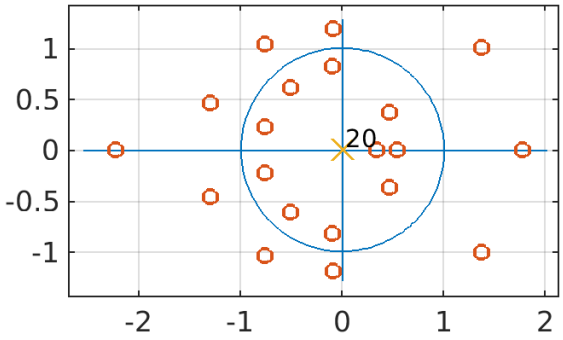

Figure 29 Pole-zero configuration for the linear phase FIR filter designed with a Bartlett window and N = 20.

Since the cosine function varies more smoothly than a linear function, Haan window tapers off more smoothly than the Bartlett window [9].

3.3.5 Blackman window

The Blackman window is defined as [22]

$$w[n] = \begin{cases} 0.42 - 0.5\cos\left(\frac{2(n+0.5)\pi}{N+1}\right) + 0.08\cos\left(\frac{4(n+0.5)\pi}{N+1}\right), 0 \le n \le N \\ 0, \text{otherwise} \end{cases} \quad (3.6)$$

Blackman window function is zero at the extreme ends of the sequence and is smoother than the Hamming window function. Figure 30 shows Blackman window function sequence for N=20 for design of example 3.1.

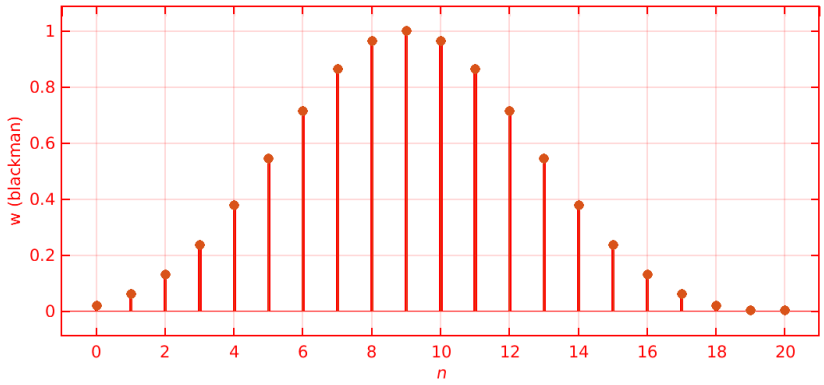

Figure 30 Blackman window function sequence for filter design with N=20.

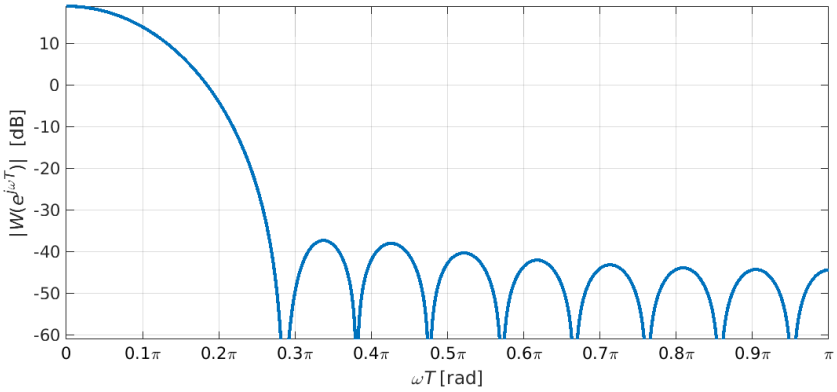

Figure 31 Magnitude responses of a Blackman window

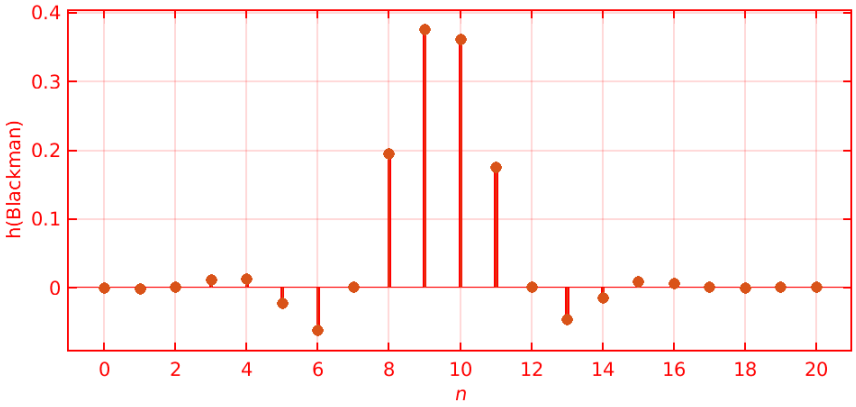

Figure 32 Impulse response of low pass filter designed using Blackman window

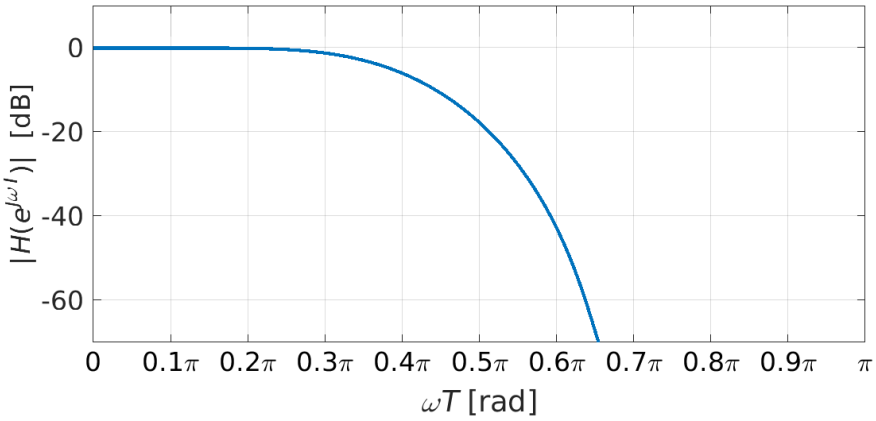

Figure 33 Magnitude responses of a linear phase FIR designed using Blackman window for design example 3.1

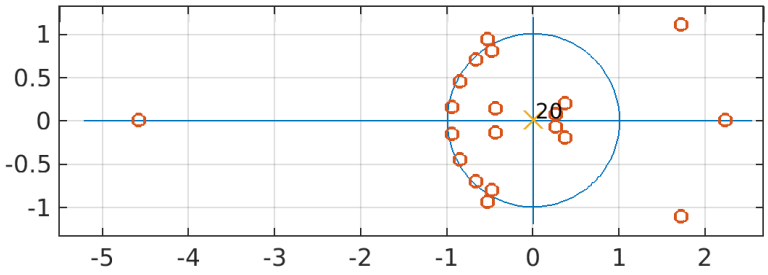

Figure 34 Pole-zero configuration for the linear-phase FIR filter designed with Blackman window and N = 20.

Filter design using this window has better stopband attenuation, but the passband response is poor. Pole-zero configuration is shown in figure 34.

3.3.6 Kaiser window

Window design can be seen as the problem of determining a time-limited function for a Fourier transform that is best the approximate of a band limited function, i.e., a time-limited function that has minimum energy outside the passband. For continuous-time function, this problem has been solved in closed form using a class of functions called prolate spheroidal wave functions [22]. Kaiser has proposed a simple approximation for the discrete-time case, the Kaiser window. The Kaiser window is an adjustable window that contains a parameter a, which can be used to trade-off between the transition width and stopband attenuation [22]. Kaiser window is defined by [22]

$$w[n] = \begin{cases} \dfrac{Io[\alpha\sqrt{1-\frac{4n^2}{(N-1)^2}}\,]}{Io\alpha}, & -\dfrac{N-1}{2} \le n \le \dfrac{N-1}{2} \quad \text{odd} \\ \dfrac{Io[\alpha\sqrt{1-\frac{4(n+0.5)^2}{(N-1)^2}}\,]}{Io\alpha}, & -\dfrac{N}{2} \le n \le \dfrac{N}{2}-1 \quad \text{even} \end{cases} \qquad 3.7$$

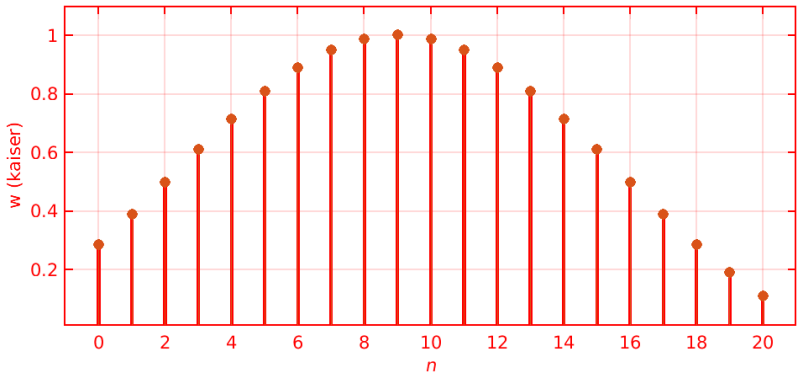

Figure 35 Kaiser window function sequence for filter design with N=20 and α = 3.4.

where, $I_o(.)$ is the zero order, modified Bessel function of the first kind. In the limiting case, when α=0 the Kaiser window reduces to a rectangular window. Figure 35 shows the Kaiser window sequence for N=20 and α = 3.4.

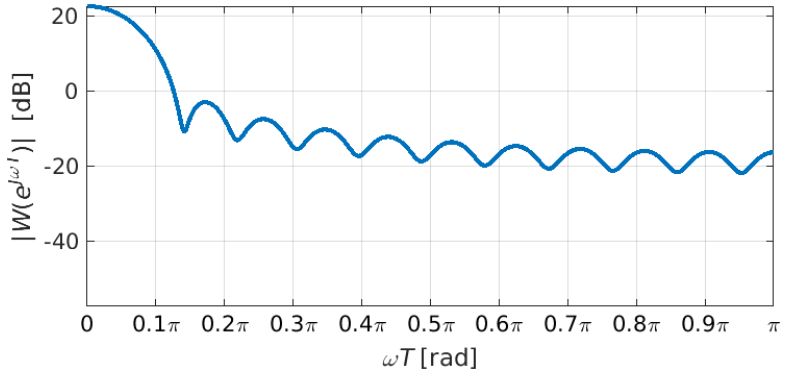

Figure 36 Magnitude responses of a Kaiser window, α = 3.4.

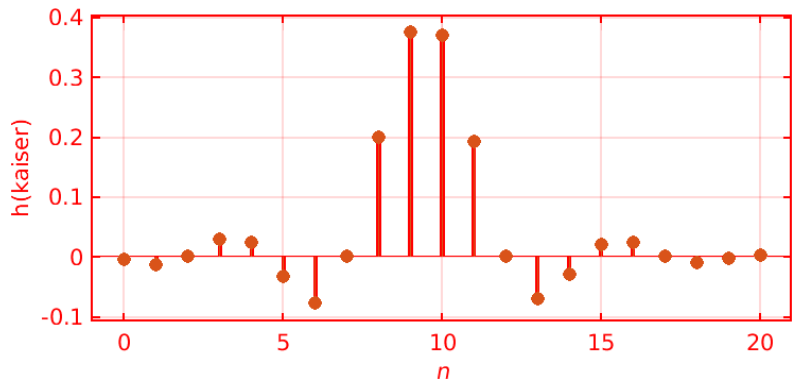

Figure 37 Impulse response of low pass filter designed using Kaiser window

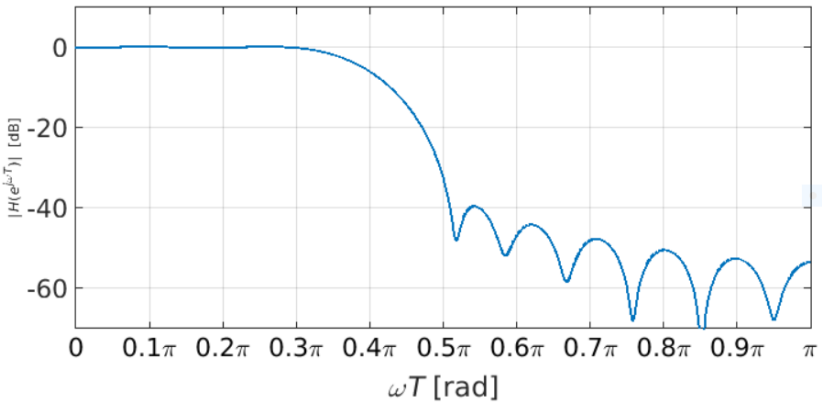

Figure 38 Magnitude responses of a linear phase FIR designed using Kaiser window for design example 3.1

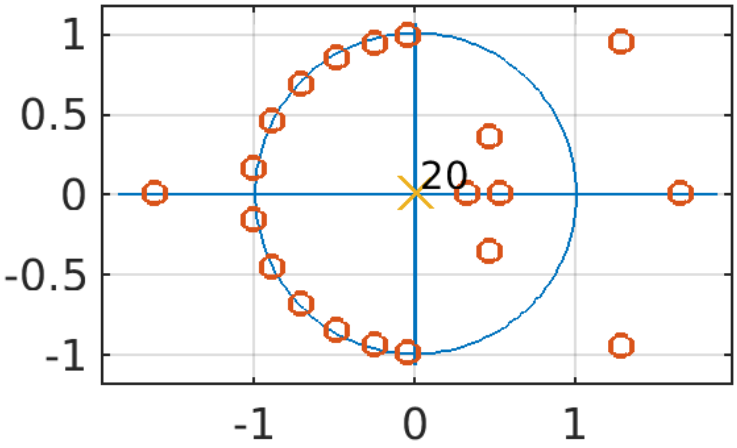

Figure 39 Pole-zero configuration for the linear-phase FIR filter designed with Kaiser window and N = 20.

Figure 38 shows the magnitude response of a linear-phase lowpass FIR filter designed with Kaiser window with N = 20 and A_{min} = 40 db. It can be noted that passband and stopband are somewhat better compared to the previously discussed windows and the transition band is slightly smaller than for the Hamming window.

Performance of all the different windows for same specification design example 3.1 has been tabulated in the table 2 below. Range of 0.35π to 0.45π has been selected as reference for evaluating stop band attenuation.

Window method	Minimum stopband attenuation (in dB)
Rectangular	21.38
Von Hann	11.63
Hamming	12.19
Bartlett	11.99
Blackman	10.54
Kaiser	13.96

Table 2 Stopband attenuation for different windows with common design specification of example 3.1.

3.3.7 Discussions of results

The design of FIR filter using windows has been discussed and the performance of various commonly used windows has been illustrated using design example 3.1. From the design example, it is observed that the rectangular window has the highest value of minimum stopband attenuation (in dB) while the Blackman window has least value among different window functions. Pole-zero configuration for all the window functions were plotted. Locations of all the poles at origin indicate absolute stability of FIR filters. Hence, FIR filters are inherently stable i.e., any bounded input results in bounded output.

Design Example 3.2: Design low pass filter with

$\omega_C T$(passband edge)=0.4π rad,

$\omega_S T$(stopband edge)=0.402π rad different using window technique.

As the order of the filter has not been specified for this design, N has been evaluated using the design procedure as illustrated in section 3.2 for different window functions. Here transition width is $\Delta\omega$ ($\omega_S T - \omega_C T$) =0.002π.

Using $\Delta\omega = 0.002\pi$ and equations from table 1, we obtain the values for filter length(N) for all the windows given in table 3.

Window method	Approximate filter length(N)
Rectangular	2000
Von Hann	4000
Hamming	4000
Bartlett	4000
Blackman	6000
Kaiser	3500

Table 3 Filter length for design example 3.2. Source section 3.2.

Rectangular window

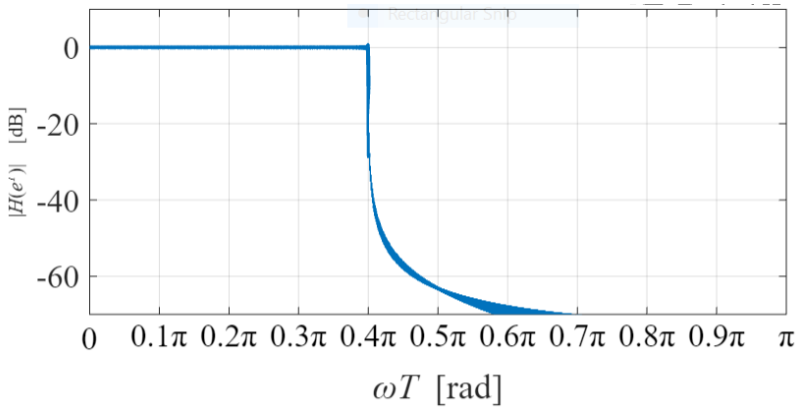

Figure 40 Magnitude response of rectangular window for design example 3.2.

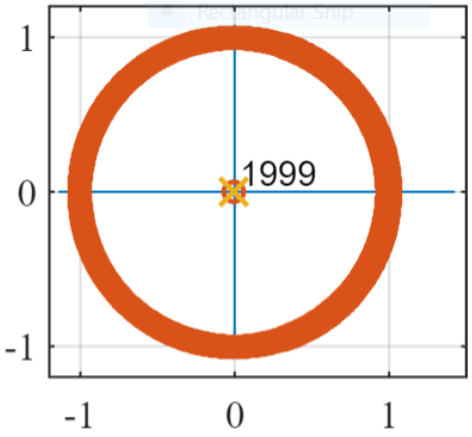

Figure 41 Pole-zero configuration of rectangular window for design example 3.2.

Von Hann window

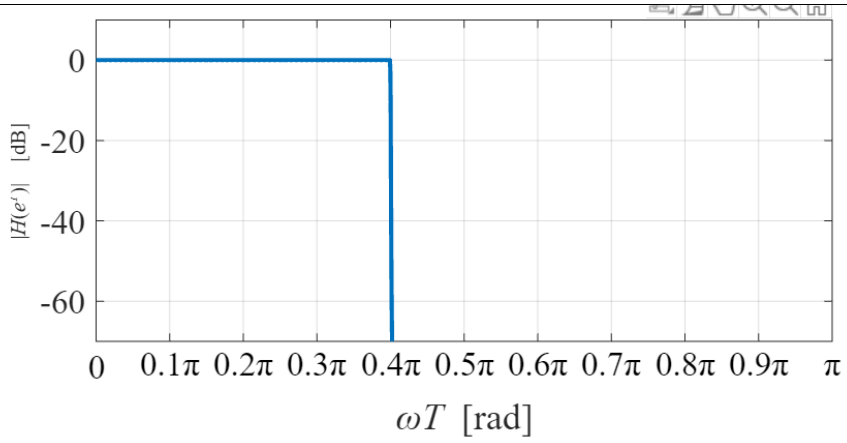

Figure 42 Magnitude response of Von Hann window for design example 3.2.

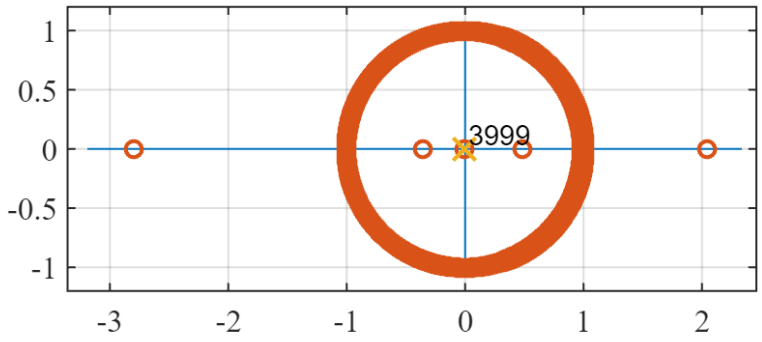

Figure 43 Pole-zero configuration of Von Hann window for design example 3.2.

Hamming window

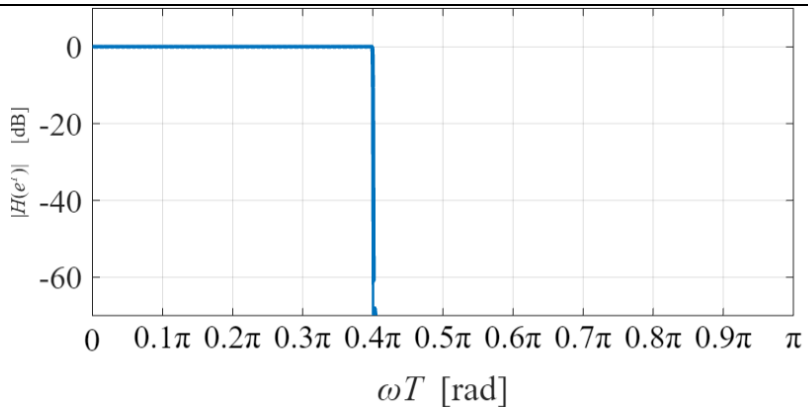

Figure 44 Magnitude response of Hamming window for design example 3.2.

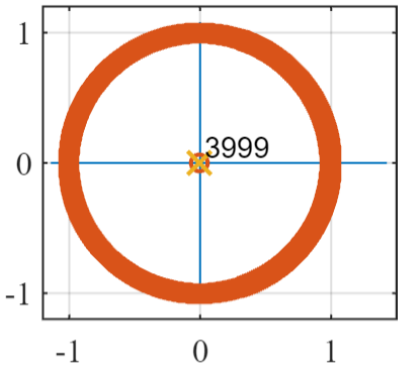

Figure 45 Pole-zero configuration of Hamming window for design example 3.2.

Bartlett window

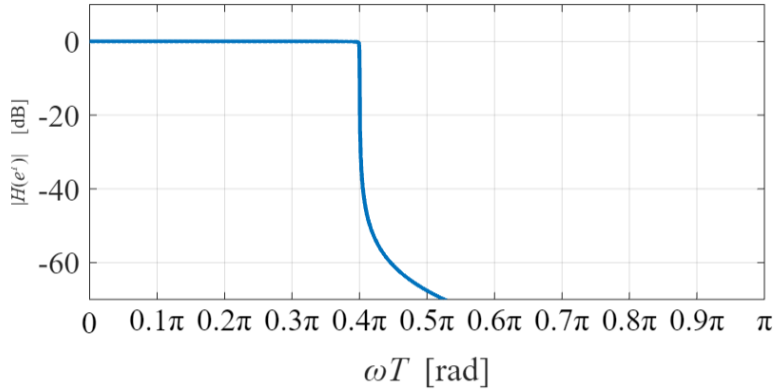

Figure 46 Magnitude response of Bartlett window for design example 3.2.

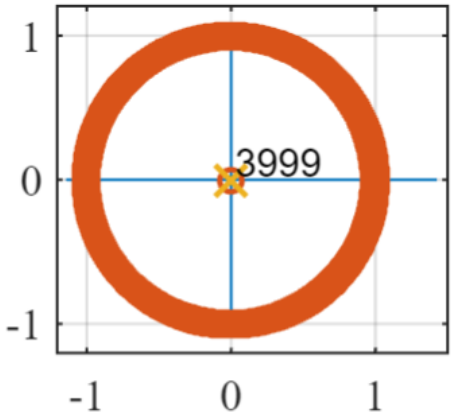

Figure 47 Pole-zero configuration of Bartlett window for design example 3.2.

Blackman window

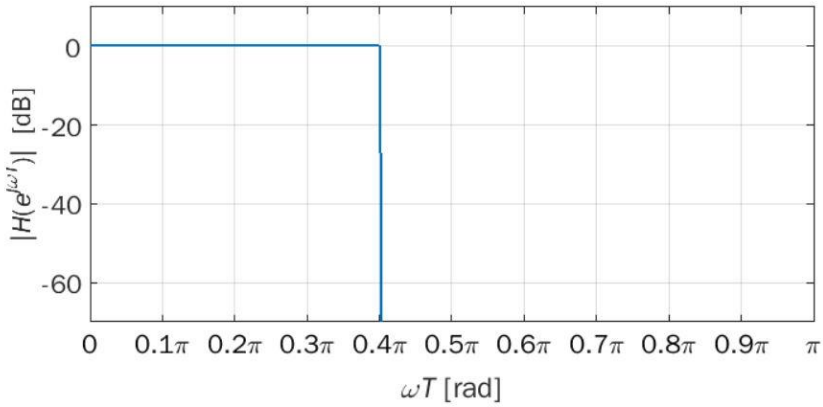

Figure 48 Magnitude response of Blackman window for design example 3.2

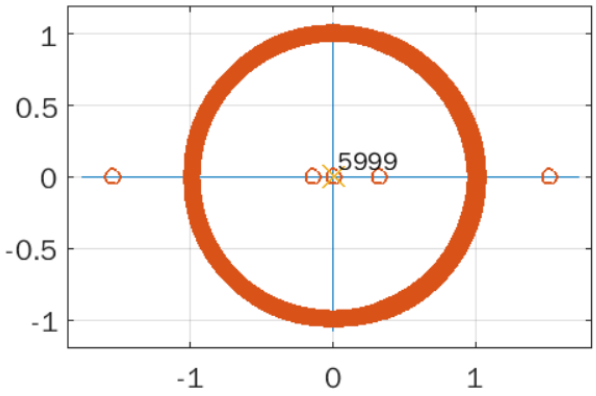

Figure 49 Pole-zero configuration of Blackman window for design example 3.2

Kaiser window

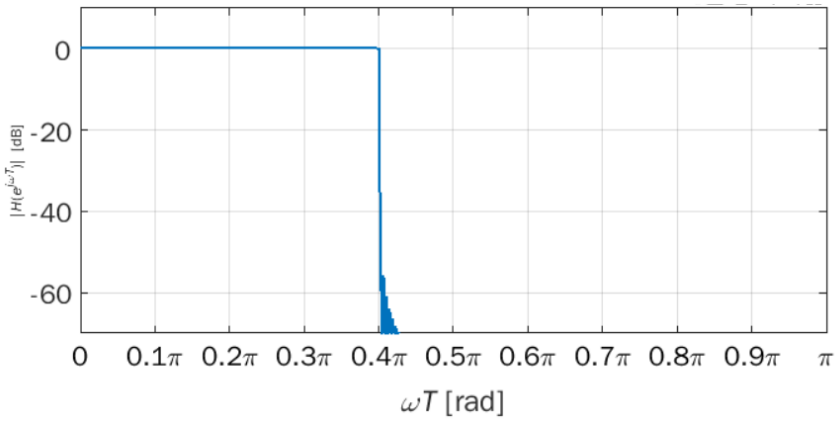

Figure 50 Magnitude response of Kaiser window for design example 3.2 with $\alpha = 3.4$.

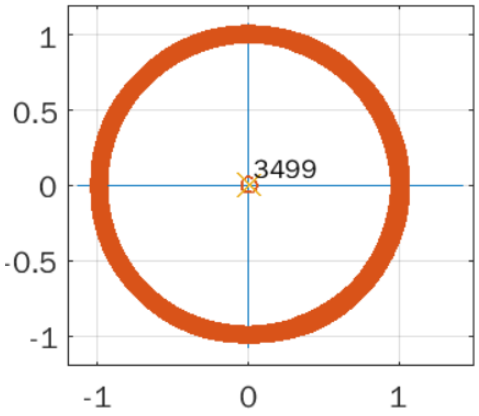

Figure 51 Pole-zero configuration of Kaiser window for design example 3.2

Stop band attenuation for example 3.2:

Window method	Minimum stopband attenuation (in dB)
Rectangular	56.47
Von Hann	48.23
Hamming	52.79
Bartlett	60.79
Blackman	62.58
Kaiser	57.27

Table 4 Stop band attenuation for design example 3.2.

3.3.8 Discussions of results for narrow transition bandwidth filter

The design of FIR Filter using windows has been discussed and the performance of various commonly used windows has been illustrated using design example 3.2 for given specification. This example shows that for design of narrow bandwidth filter, magnitude of filter length (N) is very high when window technique is applied for designing FIR filter. Traditional methods of FIR filter design are not suitable for filters which requires have very small transition bandwidth.

3.4 Summary

Two design examples were illustrated using the window technique highlighting its features and properties. The window method is easier and simpler to design with less complications but when FIR filter with narrow transition width is required, this method is not

optimal and effective as it results in higher order leading to increased arithmetic complexity and takes large computation time as compare to frequency masking method. Thus, frequency masking technique is used in such cases. Design of FIR filters based on frequency-response masking techniques, make use of periodic sub filters as basic building blocks as explained in the next subsequent sections.

Chapter 4

Design of FIR filter using frequency masking technique with one masking filter

This chapter introduces the frequency masking technique and its application for designing narrow band low pass FIR filters. The basic building blocks and structure of frequency response masking filters are discussed along with design examples.

4.1 Narrow transition band lowpass FRM FIR filter

A narrowband FIR filter (narrowband means here that $\omega_c T < \pi/2$ rad) can be realized by using two cascaded filters according to (figure 52) below. The principle is very simple: the narrow band filter is obtained as a cascade of a periodic model filter and a masking filter. The representation of up sampling has been done over one normalised time period (T).

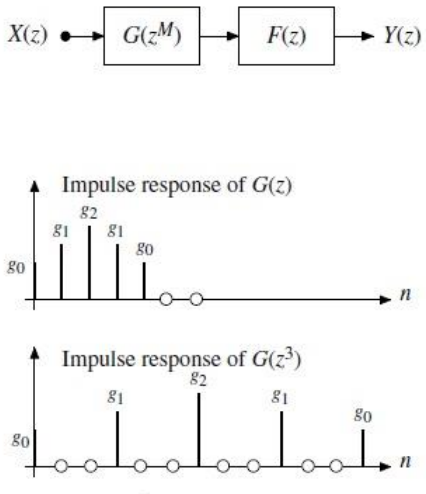

Figure 52 Up sampled. Source [22].

The overall transfer function is [22]

$$H(z) = G(z^M).\ F(z)$$

where;

G(z) : model filter

$G(z^M)$: periodic model filter

F(z) : masking filter

assuming all of them to be linear phase FIR filters. The periodic model filter $G(z^M)$ is obtained from the model filter G(z) via the transformation $z \rightarrow z^M$. The impulse response of $G(z^M)$ is obtained from the impulse response of G(z) by inserting M – 1 zeros between values, as shown in figure 52. Linear phase direct form realization of a fourth-order FIR filter is shown in figure 53. The realization of $G(z^M)$ is obtained by replacing each delay element in the realization of G(z) by M delay elements in cascade, as illustrated in figure 54.

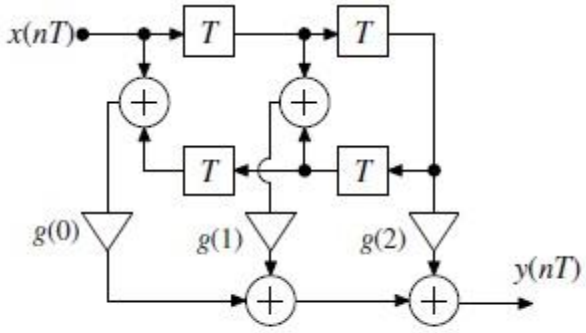

Figure 53 Realizations of G(z). Source [22].

The frequency response masking technique is more easily illustratable in the frequency domain. The response of magnitude for model, masking and overall filter have been shown below in figure 54 for M=3.

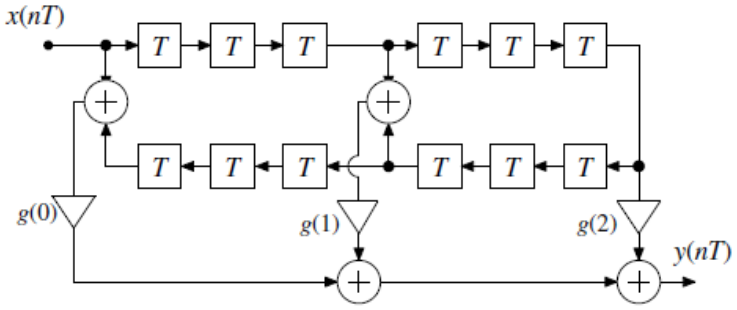

Figure 54 Realizations of $G(z^M)$ with M = 3, for a linear phase FIR filter of order four. Source [22].

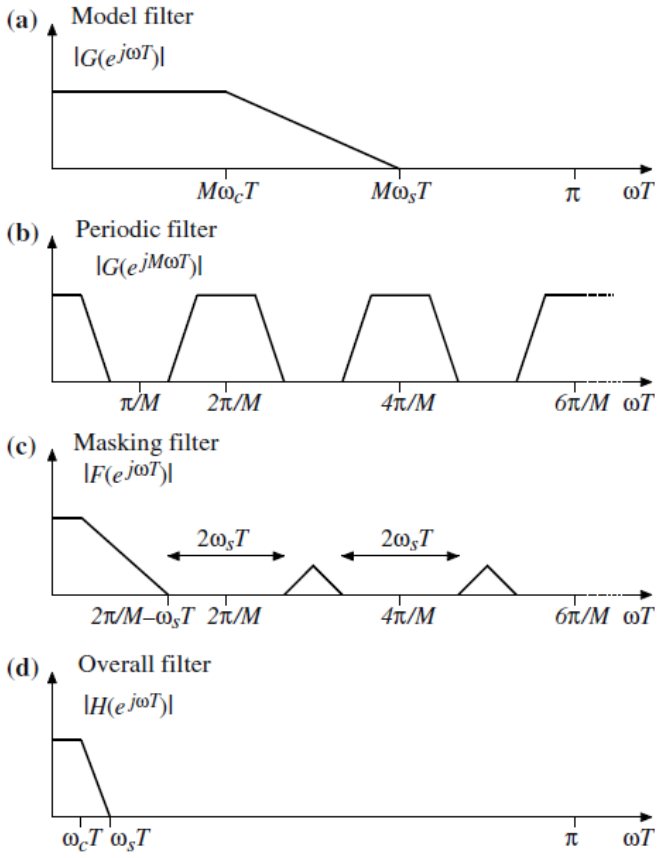

Figure 55 Magnitude response of **(a)** Model filter, (**b)** Periodic filter, (**c)** Masking filter and (**d)** Overall filter for a narrow transition band lowpass frequency masking filter. Source [22].

For narrow band low pass filter design, the model filter (G(z)) is up sampled by a factor M resulting a periodic model filter ($G(z^M)$). This interpolation by a factor M in time

domain leads to compression of magnitude response in frequency domain for the model filter. The masking filter (F(z)) is periodic in nature [22]. The periodic model filter and the masking filter are shown in figure 55(b) and figure 55(c) respectively. The periodic model filter is cascaded with the masking filter and the magnitude response of both the periodic model filter and the masking filter are multiplied resulting in a magnitude response of narrow transition band low pass filter. The magnitude response of the overall filter is shown in figure 55(d).

4.2 Design constraints and steps

The aim is to design a lowpass filter H(z) with passband and stopband edges at $\omega_c T$ and $\omega_s T$, respectively. This design in based on [26]. Given the specification parameters passband frequency ($\omega_c T$), stopband frequency ($\omega_s T$), passband ripple(δ_c) and stopband ripple(δ_s)

Steps 1: First step is to design the model filter G(z) to have band edges at $M\omega_c T$ and $M\omega_s T < \pi$ rad, as shown in figure 55(a) [26].

Step 2 : $G(z^M)$ is obtained from G(z) through the transformation $z \rightarrow z^M$. The magnitude response of $G(z^M)$ is obtained from G(z), and is periodic with a period of $2\pi/M$ instead of 2π. In other words, $G(e^{jM\omega T})$ merely is M times compressed versions of $G(e^{j\omega T})$. Hence, $G(z^M)$ contains the desired passband at lower frequencies but also some unwanted images of this passband as shown in figure 55(a) [26].

Step 3 : Masking Filter F(z) is cascaded with $G(z^M)$ to extract the desired passband and suppress the unwanted images, as shown in figure 55. The overall lowpass filter H(z) is shown in figure 55 (d) [26]. It is periodic in nature [26].

The passband ripple of the overall filter H(z) is in the worst case the sum of the passband ripples of F(z) and $G(z^M)$ with this reasoning the passband ripple of these filters has been allowed to be half that of the overall filter. Further, if F(z) and $G(z^M)$ have a specific stopband ripple, then H(z) is ensured to have the same, or smaller, stopband ripple [26].

With the above mentioned arguments, following design constraints are obtained for overall, model and masking filter [22]:

Desired response:

$$1 - \delta_c \leq \left|H\left(e^{j\omega T}\right)\right| \leq 1 + \delta_c\ ,\ \omega T \in [0, \omega_c T]$$
$$\left|H\left(e^{j\omega T}\right)\right| \leq \delta_s\ ,\ \omega T \in [\omega_s T, \pi] \quad (4.1\text{- a})$$

Model filter:

$$1 - \delta_c^{(G)} \leq \left|G\left(e^{j\omega T}\right)\right| \leq 1 + \delta_c^{(G)}\ ,\ \omega T \in [0, M\omega_c T]$$
$$\left|G\left(e^{j\omega T}\right)\right| \leq \delta_s^{(G)}\ ,\ \omega T \in [M\omega_s T, \pi] \quad (4.1\text{- b})$$

Masking filter:

$$1 - \delta_c^{(F)} \leq \left|F\left(e^{j\omega T}\right)\right| \leq 1 + \delta_c^{(F)}\ ,\ \omega T \in [0, \omega_c T]$$
$$\left|F\left(e^{j\omega T}\right)\right| \leq \delta_s^{(F)}\ ,\ \omega T \in [\ \Omega_s] \quad (4.1\text{- c})$$

where the stopband region Ω_s of the masking filter is [22]

$$\Omega_s = \bigcup_{k=1}^{\left\lfloor \frac{M}{2} \right\rfloor} [k\frac{2\pi}{M} - \omega_S T,\ \min\ (k\frac{2\pi}{M} + \omega_S T,\ \pi)] \quad (4.2)$$

Ω_s indicates the stopband region for masking filter. In this region the magnitude of masking filter (F(z)) is less than the permissible stopband ripple. It is possible to reduce the complexity considerably by simultaneously optimizing G(z) and F(z) [22].

Design example 4.1: Narrow transition band low pass filter designed with following specifications:

$\omega_C T = 0.045\pi$ rad

$\omega_S T = 0.05\pi$ rad

$\delta_C = 0.01$

$\delta_s = 0.001$

Parks,MaClellan and Rabinar [32] algorithm have been used in desinging of model filter G(z) and masking filter F(z). To find the optimum value of M that minimizes the overall complexity, plotting of the estimated filter length(N) for the model(G(z)), masking(F(z)) and overall filter(H(z)) using MATLAB with design constraints i.e., equation 4.1 and 4.2. Plot has been shown in figure 56. This plot shows the filter length (N) for the two filters as well as the overall filter length (H(z)). Filter length of G(z) and F(z) are obtained as [22]

$$N_G \approx \frac{-4\pi \log_{10}(13\delta_c^{(G)}\delta_s^{(G)}}{3\,M(\omega_s T-\omega_c T)}$$

$$N_F \approx \frac{-4\pi \log_{10}(13\delta_c^{(G)}\delta_s^{(G)}}{3\,(\frac{2\pi}{M}-(\omega_s T+\omega_c T))} \qquad (4.3)$$

Considering passband ripple of G(z) and F(z) being equal i.e., 0. 005.After finding the optimized M from plotting result, implying that minimum occurs at M= 10(from figure 56), Then G(z) and F(z) are designed with the design constraints expressed in equation 4.1 to 4.2.

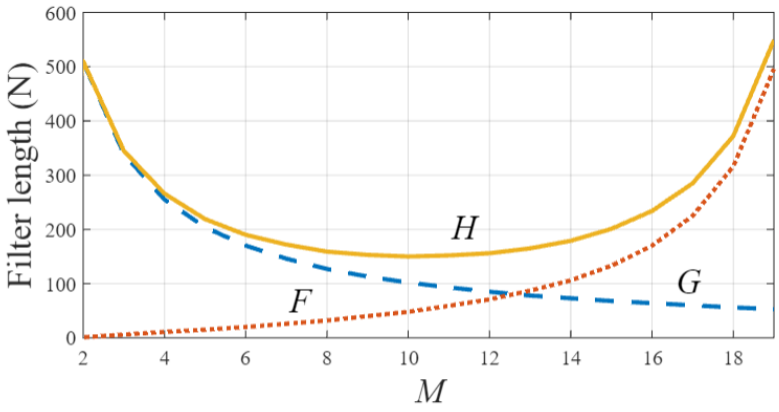

Figure 56 Filter length for the model (dashed lines), masking filter (dotted line), and overall filter (solid lines).

Plot of filter length (N) against different values of the up-sampling factor (M) has been shown in the figure 56. The filter length has been evaluated for masking filter(F(z)) and model filter(G(z)) using equation 4.3. For up-sampling factor of M=10, filter length of the model filter is 62 while filter length of masking filter is 57. The filter length of overall filter is 677.

Magnitude responses of the model and periodic filters are shown in figure 57 and figure 58 respectively, below

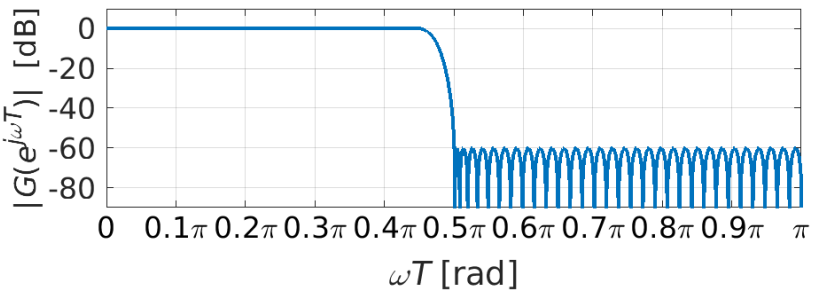

Figure 57 Magnitude response of model filter

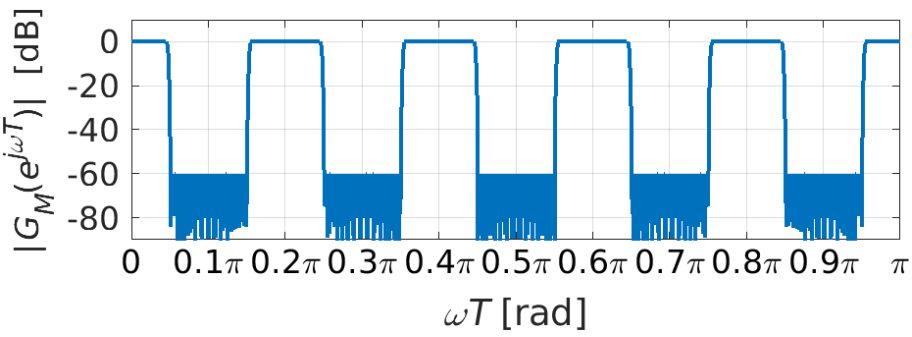

Figure 58 Magnitude response of periodic model filter

The magnitude response of the masking and the overall filter are shown in figure 59 and figure 60 respectively, below

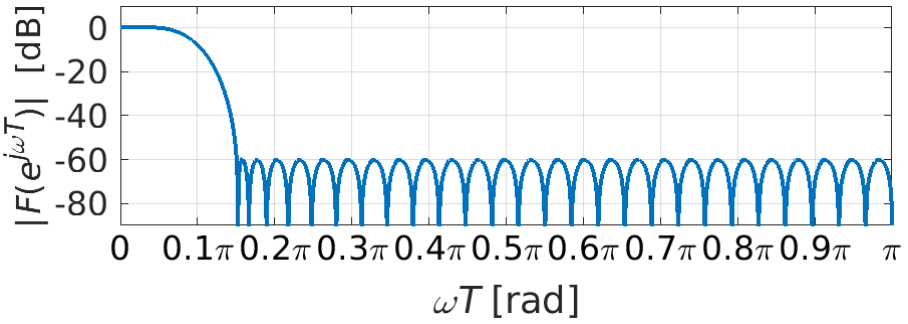

Figure 59 Magnitude response of masking filter

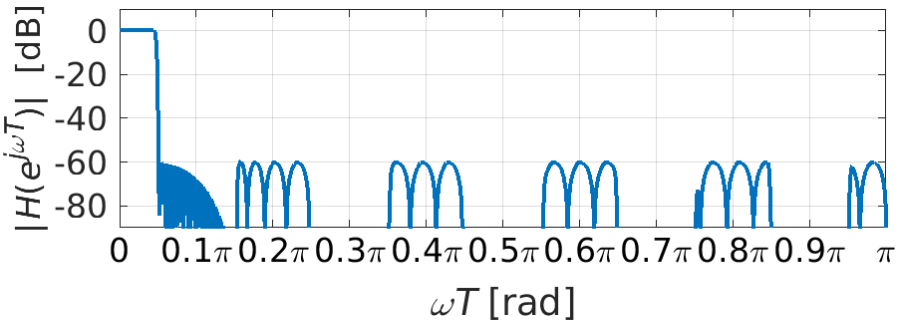

Figure 60 Magnitude response of overall filter

For the same specifications of design example 4.1, the approximate filter length (N), the stop band attenuation (A_S) is evaluated in table 5, for a filter designed using the window method with transition width ($\Delta\omega$) 0.005π.

Window method	Approximate filter length(N)	Minimum stopband attenuation (in dB)
Rectangular	800	23.87
Von Hann	1600	18.57
Hamming	1600	17.69
Bartlett	1600	18.25
Blackman	2400	16.41
Kaiser	2300	21.94
FRM Method	**Approximate filter length(N)**	**Minimum stopband attenuation (in dB)**
Frequency Masking technique	677	27.77

Table 5 Filter length and stop band attenuation of example 4.1 designed with using window technique. Source section 3.2

For the same specification design for example 4.1, window method requires much higher order than the masking technique which requires only 677. Thus, reducing the arithmetic complexity and computation. As a simple measure of arithmetic complexity is the number of multiplications per sample [22]. As discussed in earlier sections the order of an FIR filter is roughly inversely proportional to the transition bandwidth. The order and arithmetic complexity of the model filter G(z) is, therefore, lower than that for a conventional filter since its transition bandwidth is M times wider. The complexity of the masking filter F(z), on the other hand, increases with M, but if this number is chosen correctly, then the transition band of F(z) becomes wider, which results in a low complexity for this filter as well. Hence the overall complexity is significantly reduced.

The optimum value of M that minimizes the overall complexity can be found by plotting the total complexity of different choices of M, as shown in design example 4.1. The price to pay for the reduced arithmetic complexity is that the number of delay elements and overall delay is increased somewhat, mainly due to the masking filter.

4.3 Summary

Low pass FIR filter design using the frequency masking technique was presented and it was shown that there is a reduction in order with respect to the window method resulting in less arithmetic complexity and computations. This method can only be used for the filters with limits on the bandwidth depending on M (up-sampling factor). This limitation has been resolved in next chapter, where two masking filters are used instead of one masking filter.

Chapter 5

Design of FIR filter using frequency masking technique with two masking filters

In this chapter the design of lowpass FIR filters by applying the frequency masking technique with two masking filters (sub filters) is discussed. The filter design constraints and the steps which are involved in this design method are discussed. At the end a comparison of the frequency masking technique with the window method is done.

5.1 Introduction

An up-sampled FIR filter uses multiple sample delays between the taps, compared to the unity delays in a conventional FIR filter. The resulting frequency response has steeper edges, but contains periodic images along the frequency axis (figure 61).

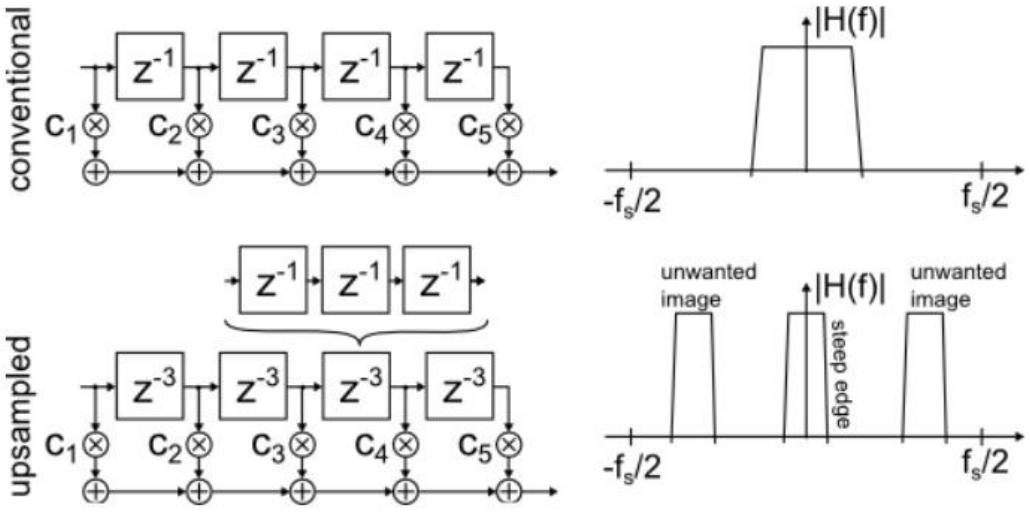

Figure 61 Conventional and up-sampled FIR. Source [23]

A complementary filter is constructed from the up sampled filter by subtracting its output from a unity impulse response with the same group delay (conveniently derived

from the same tapped delay line at no extra cost). Then the up-sampled filter has a passband, where the complementary filter shows a stopband, and vice versa.

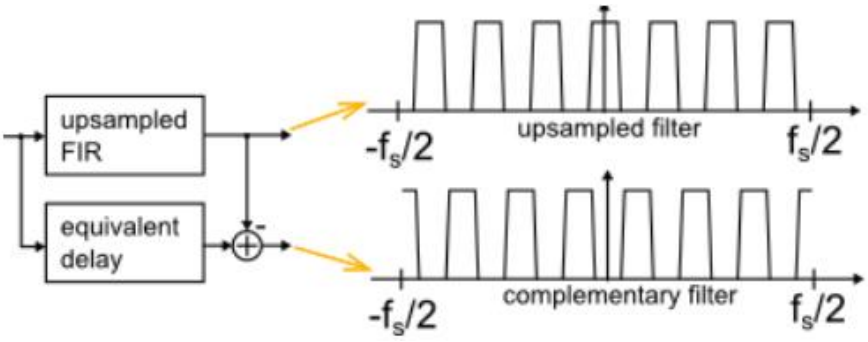

Figure 62 Up-sampled and complementary FIR. Source [23]

Subsequently a FIR masking filter 1 and a masking filter 2 are added to the outputs, and the results are summed (figure 63). This is the basic topology of the frequency-masking FIR filter:

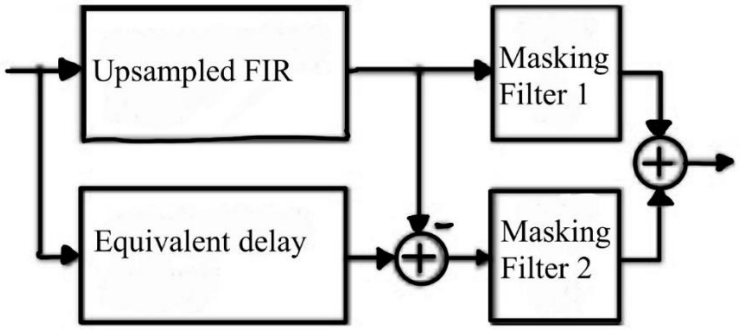

Figure 63 Frequency masking FIR filter. Source [23]

5.2 Structure and frequency response of FRM filter

A basic FRM filter [1] consists of four modules that are connected in parallel as shown in figure 64. It involves a linear phase prototype filter $H_a(z)$ that up-samples the input signal by M, a pair of linear phase masking filters $\{F_0(z)$ and $F_1(z)\}$, and a delay line. All three sub-filters involved, namely, $H_a(z)$, $F_0(z)$, and $F_1(z)$ are linear phase FIR filters of length N_a, N, and N_c, respectively.

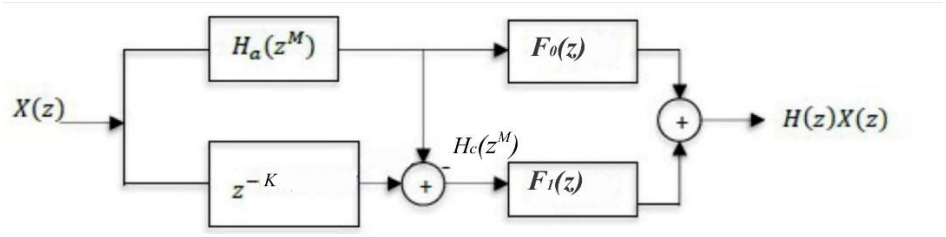

Figure 64 Structure of a filter synthesized using frequency masking filter. Source [22]

The transfer function of the FRM filter is obtained as [1]

$$H(z) = H_a(z^M).\ F_0(z)+H_c(z^M).\ F_1(z) \quad (5.1)$$

where,

$K = \frac{(N_a-1)*M}{2}$ is group delay of $H_a(z^M)$

$$H_c(z^M)=z^{-K} - H_a(z^M) \quad (5.2)$$

hence,

$$H(z) = H_a(z^M).\ F_0(z)+[\ z^{-K} - H_a(z^M)].\ F_1(z) \quad (5.3)$$

where,

$$H_a(z^M) =\sum_{k=0}^{Na} h_k\, z^{-kM} \quad (5.4)$$

$$F_0(z) = \sum_{k=0}^{N} h_k^{(a)}\, z^{-k} \quad (5.5)$$

$$F_1(z) = \sum_{k=0}^{Nc} h_k^{(c)}\, z^{-k} \quad (5.6)$$

Based on (5.1), the zero phase frequency response of the FRM filter is given by [22]

$$H(e^{j\omega})= H_1(e^{j\omega}) + H_2(e^{j\omega})$$

where

$$H_1(e^{j\omega}) =H_a(e^{jM\omega}).F_0(e^{j\omega}) \quad (5.7)$$

and $H_2(e^{j\omega}) =[1-H_a(e^{jM\omega+K}).F_1(e^{-jK\omega})$

From (5.1) to (5.7), it is evident that filters $H_a(z)$ and $H_c(z)$ form a complementary pair because $|H_a(e^{j\omega}) + H_c(e^{j\omega})| =1$.

5.3 The role of complementary pair {$H_a(z)$, $H_c(z)$}

Two linear phase filter $H_a(z)$ and $H_c(z)$ are said to be a complementary pair if $|H_a(e^{j\omega}) + H_c(e^{j\omega})| = 1$,where $H_a(e^{j\omega})$ and $H_c(e^{j\omega})$ are frequency response respectively.

For the prototype filter H(z), the frequency response can be expressed as

$$H_a(e^{j\omega}) = e^{-j(\frac{N-1}{2})\omega} A(\omega)$$

Here A(ω) is a trigonometric function of ω. [20], [21] N-1 is even here. Consider a typical case where $H_a(z)$ is a lowpass filter whose magnitude response is illustrated in figure 65(a) where θ and ϕ are passband and stopband edges, respectively. The magnitude response of $H_c(z)$, which is known to be complementary to $H_a(z)$, is depicted in figure 65(b). When a filter is up-sampled by M and the complementary pair is used, namely$\{H_a(e^{j\omega}), H_c(e^{j\omega})\}$, the frequency responses are$\{H_a(e^{jM\omega}), H_c(e^{jM\omega})\}$.Typically, integer M here is considerably greater than unity, and so over the normalized frequency [- π, π], the frequency responses $H_a(e^{jM\omega})$ and $H_c(e^{jM\omega})$=1-$H_a(e^{jM\omega})$ becomes a total of M "squeezed (that is M times narrower)" copies of $H_a(e^{j\omega})$and 1-$H_a(e^{j\omega})$, respectively.

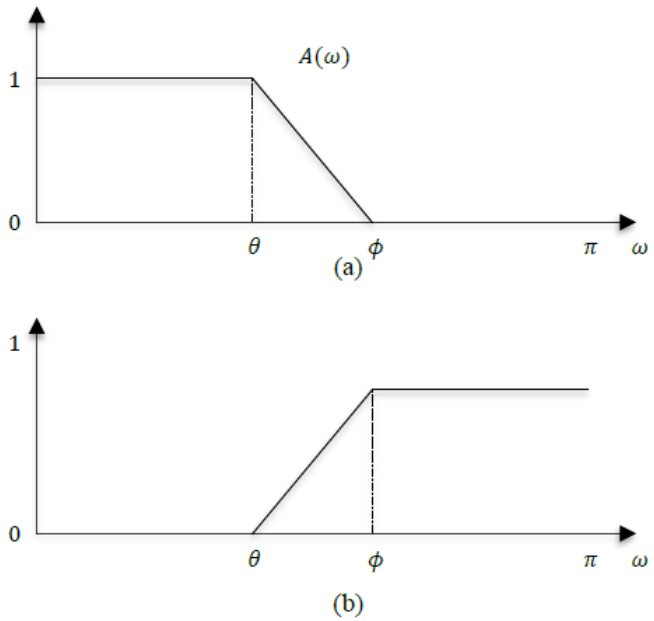

Figure 65 Zero-phase frequency response of (a) $H_a(z)$ and (b) $H_c(z)$. Source [1]

As a result, each individual copy of these squeezed copy possesses shorter passband/stopband and sharper transition band, and still remains complementary. See the first two subplots in figure 66 and figure 67 for illustration in this regard [10].

5.4 Role of masking filters $F_0(z)$ and $F_1(z)$

Figure 66 and figure 67 illustrate the cases of broad-passband and narrow-passband lowpass FRM filters, respectively. In the case of designing a broad passband lowpass FRM filter (see figure 67), the passband and stopband edges of overall transfer function (H(z)) are given by [18] [29]

$$\omega_P = \frac{2\pi m + \theta}{M} \qquad (5.8\ a)$$

and

$$\omega_S = \frac{2\pi m + \phi}{M} \qquad (5.8\ b)$$

Where m is an integer less than M and θ, ϕ is shown in figure 66 (d). From (5.8), it follows that the transition band of the FRM filter is equal to $(\phi - \theta)/M$ and for M>1 it is narrower than that of the prototype lowpass filter $H_a(z)$. By using the lowpass masking filters $F_0(z)$ and $F_1(z)$ with appropriate passbands (that are shown in plots (a) and (b) of figure 66 as dashed lines), it can be observed that only the first section of the complementary pair $H_a(e^{j\omega})$ and $(1- H_a(e^{j\omega}))$ survives and, as shown in plots (c) and (d) of figure 66, when the two channels are added up, a lowpass filter with flat and broad passband and sharp transition band is produced. It can be noted that the group delay of masking filters $F_0(z)$ and that of $F_1(z)$, should be equal in order for them to perform frequency-response masking effectively. This means that the length of $F_0(z)$ and $F_1(z)$ either be both odd or both even and, if necessary leading delays must be added to either F_0 or F_1, to equalize their group delays. Also note that in order to avoid half sample delay $(N - 1)$ must be even.

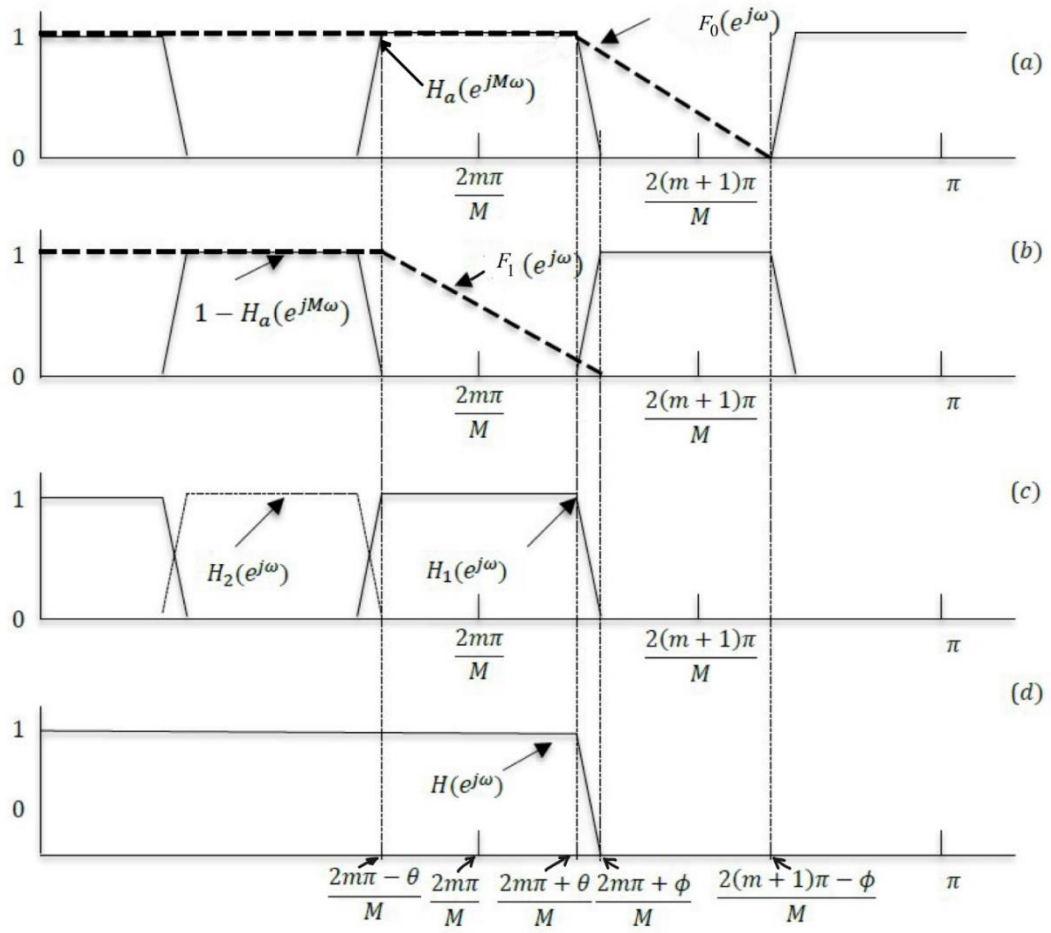

Figure 66 Low pass FRM filter with broad passband. Source [1]

As Figure 67 shows, FRM structure can also be utilized to construct a lowpass filter with relatively narrow passband and a sharp transition band. This is achieved by using a lowpass prototype filter with narrow passband and, at the same time, employing lowpass masking filters with appropriate passbands. In the case of narrow band, passband and stopband edges, denoted again by ω_p and ω_s {shown in figure 67(d)}, for overall transfer function (H(z)) are given by [18] [29]

$$\omega_p = \frac{2\pi m - \phi}{M} \qquad (5.9\ a)$$

and

$$\omega_s = \frac{2\pi m - \theta}{M} \qquad (5.9\ b)$$

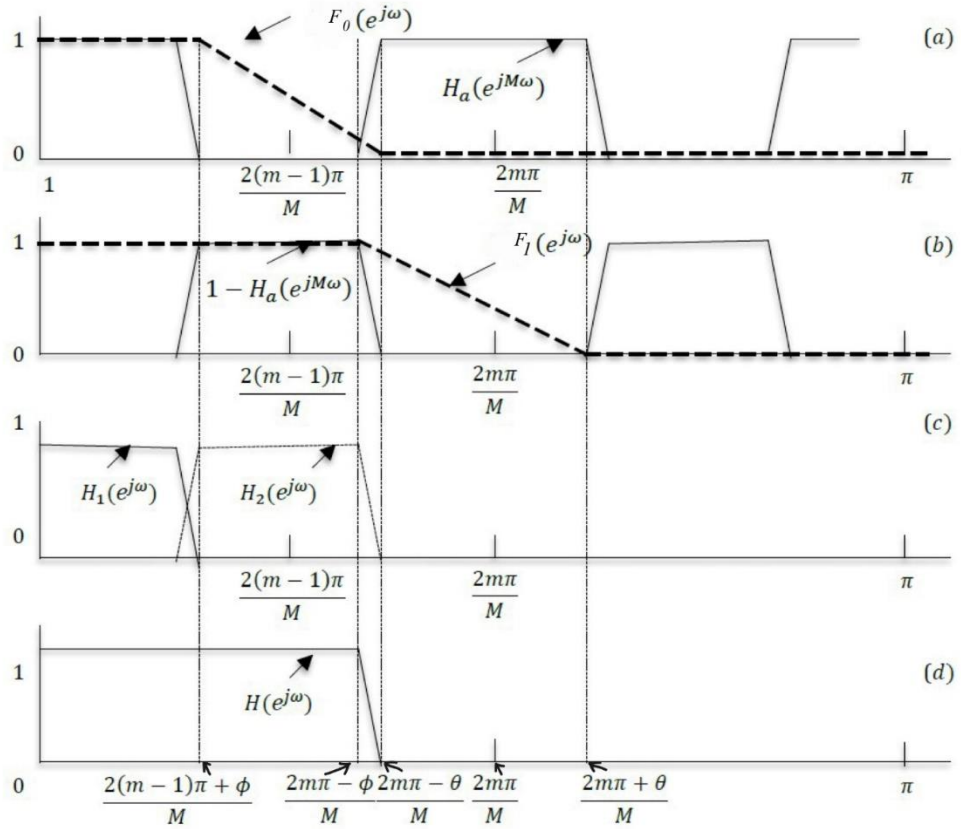

Figure 67 Low pass FRM filter with narrow passband. Source [1]

In order to design a narrow band low pass filter using a model filter $H_a(z)$ and masking filters ($F_0(z)$ and $F_1(z)$), complementary pair of $H_a(z^M)$ is designed using up sampling by the factor K(in equation 5.2).The magnitude responses of masking filters $F_0(z)$ and $F_1(z)$ are shown with dashed lines in figure 66 and figure 67. The magnitude response product of the up sampled model filter $H_a(z^M)$ concatenated with masking filter $F_0(z)$ gives the magnitude response of $H_1(z)$. Similarly, magnitude response product of complementary model filter $H_C(z^M)$ ($H_C(z^M)$ = 1- $H_a(z^M)$) with masking filter $F_1(z)$ gives $H_2(z)$. Summation of magnitude response of $H_1(z)$ and $H_2(z)$ gives overall response of filter H(z) shown in figure 66(d) and figure 67 (d).

5.5 Arbitrary bandwidth FRM FIR filter

Using two masking filters {$F_0(z)$ and $F_1(z)$}, it is possible to better control the bandwidth. The above discussion shows that was not possible using the technique explained in the previous chapter 4. In this chapter, the overall filter makes use of a periodic model filter, its delay-complementary filter, and two masking filters. By using this approach, it is possible to obtain filters with low complexity for arbitrary bandwidths.

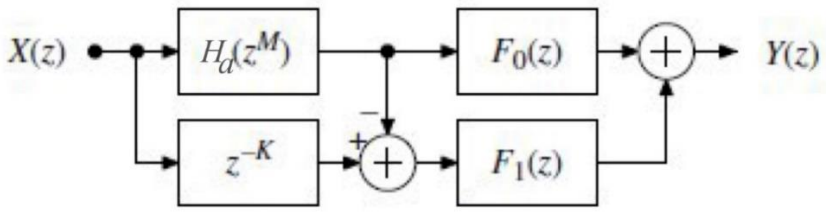

Figure 68 Arbitary bandwidth FIR FRM filter.Source[1]

Overall transfer function is :

$$H(z)= H_a(z^{M)}\cdot F_0(z) + H_C(z^M)F_1(z) \qquad (5.10)$$

All filters are here linear phase FIR filters.

$H_a(z^M)$: - periodic model filter

$H_C(z^M)$:- Delayed complementary periodic model filter

$F_0(z)$
$F_1(z)$ } Masking filters

The delay-complementary filter $H_C(z^M)$ is given by

$$H_C(z^M) = z^{-K} – H_a(z^M) \qquad (5.11)$$

K is group delay of $H_a(z^M)$,filter is realised using the scheme shown in figure 68.

The delay-complementary filter of $H_a(z^M)$ is found by subtracting pure delay, $z^{–K}$, where $K = (N_a\text{-}1).M/2$, from $H_a(z^M)$ where N_a is the filter length of $H_a(z)$. Hence, to get an integer delay, N_a is chosen to be even length. The masking filters extract one or several passbands of the periodic model filters, respectively. For a lowpass filter design, typical magnitude responses of the model, masking, and overall filters are shown in figure 69 and figure 70. The transition band of the overall filter equals the transition band of either $H_a(z^M)$ or $H_c(z^M)$,equation 5.11.

The masking filters $F_0(z)$ and $F_1(z)$ are linear-phase FIR filters with the same group delay. Hence, if one filter is shorter than the other, then the shorter filter should be padded with zeros to make them have equal group delays. The two filters may be either of even or odd orders. For the lowpass case the model filter and the masking filters are designed to be low pass filters.

Case 1) When overall transition is determined by $H_a(z^M)$: Considering $\omega_c T$ and $\omega_s T$ to be passband and stopband edges of the overall filter H(z) respectively, from figure 69 (d), then passband and stopband edges of the model filter $H_a(z)$ for the case dominated by $H_a(z^M)$ is shown with upper subscript on the parameter [22]:

$$\omega_c^{Ha} T = M\omega_C T - 2k\pi \qquad (5.12)$$

And

$$\omega_S^{Ha} T = M\omega_S T - 2k\pi \qquad (5.13)$$

For lowpass filter designing $0 < \omega_C T < \omega_S T < \pi$ rad and $k = \left\lfloor \frac{M\omega_c T}{2\pi} \right\rfloor$.

The M_{opt} that minimizes the arithmetic complexity in terms of the number of multiplications is [22]

$$M_{opt} = \frac{1}{\sqrt{\frac{2\beta}{\pi}(\omega_s T - \omega_c T)}} \qquad (0 < \omega_C T < \omega_S T < \pi \text{ rad}) \qquad (5.14)$$

where $\beta = 1$ if the sub filters are optimized separately, and $\beta = 0.6$ if the sub filters are optimized jointly.

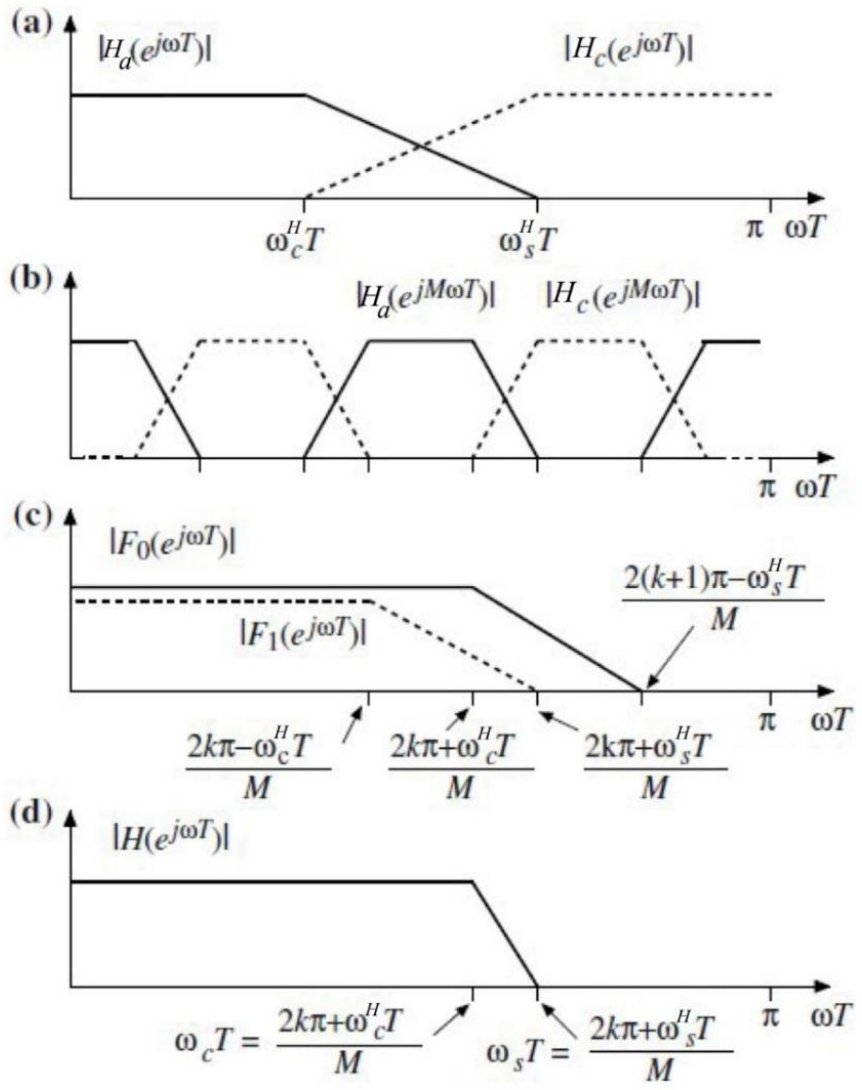

Figure 69 Magnitude response for arbitary bandwidth frequency masking filter when overall bandwidth is determined by $H_a(z^M)$ **(a)**Model and complementary model filters ,**(b)** Their periodic counter parts ,**(c)** Masking filters and (**d)** Overall filter. Source [22].

Case 2) When overall transition is determined by $H_C(z^M)$: Considering $\omega_C T$ and $\omega_S T$ are passband and stopband edges of the overall filter H(z) respectively. Then from figure 70(d), passband and stopband edges of the model filter $H_a(z)$ for the case dominated by $H_c(z^M)$ (shown with upper subscript on the parameter) is given by :

$$\omega_c^{Hc} T = 2k\pi - M\omega_C T \quad (5.15)$$

and

$$\omega_S^{Hc} T = 2k\pi - M\omega_S T \quad (5.16)$$

For lowpass filter designing $0<\omega_C T<\omega_S T<\pi$ rad and $k = \left\lceil \frac{M\omega_S T}{2\pi} \right\rceil$. The transition band of $\omega_s^H T - \omega_c^H T = M(\omega_s T - \omega_c T)$ and the sum of the transition band of $F_0(z)$ and $F_1(z)$ is $2\pi/M$. Hence, the complexity of H(z) decreases with increasing M, while the complexity of $F_0(z)$ and $F_1(z)$ increases with increasing M. The M_{opt} that minimizes the arithmetic complexity in terms of the number of multiplications is given in equation 5.14.

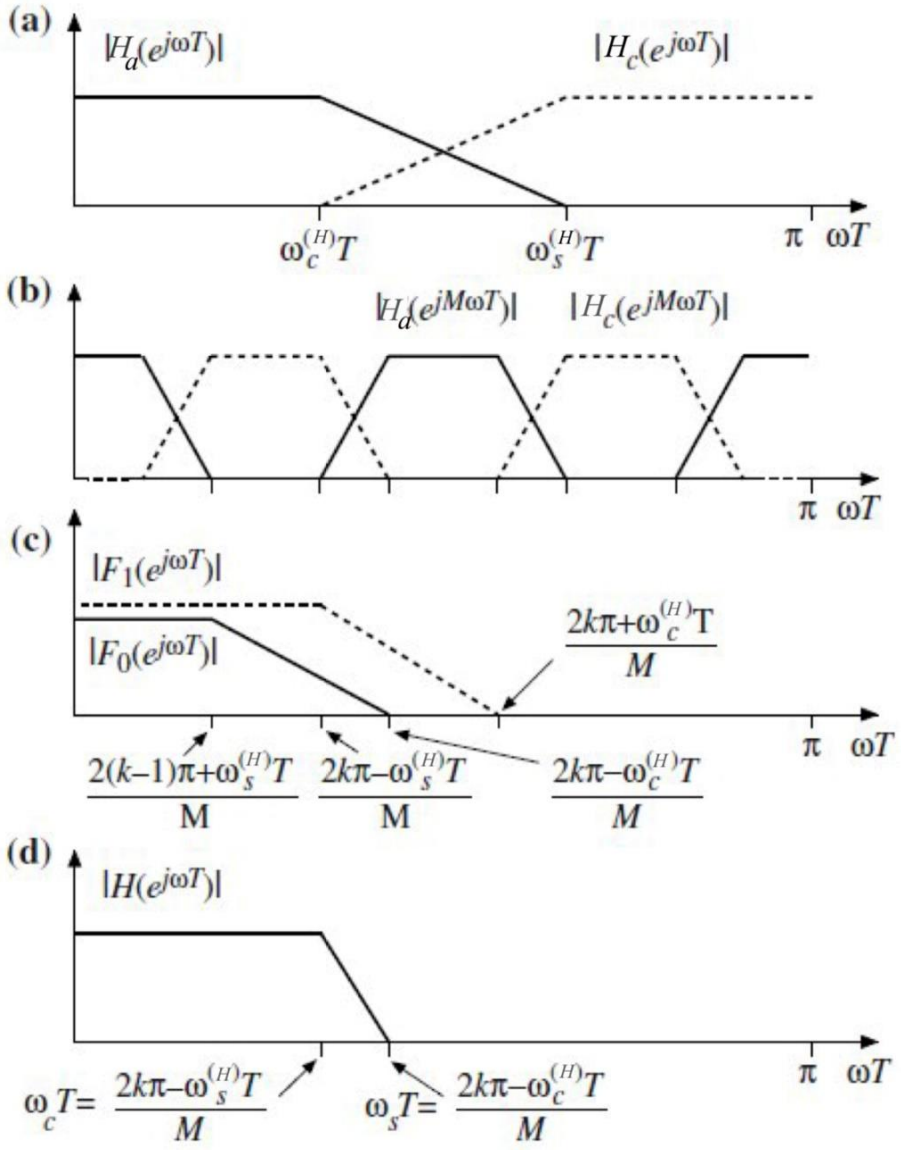

Figure 70 Magnitude response for arbitary bandwidth frequency masking filter when overall bandwidth is determined by $H_C(z^M)$ **a)** Model and complementary model filters, **b)** Their periodic counter parts ,**c)** Masking filters and **d)** Overall filter. Source [22].

Design constraints:

Design procedure without joint optimization is:

1) Determine the optimum M which minimizes the complexity according to equation 5.14.
2) Finding the passband and stopband edge of the model filter $H_a(z)$ according to equation 5.12 and 5.13 for case 1 or for case 2 using equation 5.15 and 5.16.
3) For case 1, when the overall bandwidth is determined by $H_a(z^M)$, passband and stopband edge of the masking filter $F_0(z)$ are designed using $(2k\pi + \omega_c{}^H T)/M$ and $([2(k+1)\pi - \omega_s{}^H T]/M)$ respectively. The passband and stopband edge of the masking filter $F_1(z)$ is $(2k\pi - \omega_c{}^H T)/M$ and $(2k\pi + \omega_s{}^H T)/M$ respectively. M is determined form step 1 and k = $\left\lfloor \frac{M\omega_c T}{2\pi} \right\rfloor$
4) For case 2, when the overall bandwidth is determined by $H_c(z^M)$, passband and stopband edge of the masking filter $F_0(z)$ are designed using $(2k\pi - \omega_c{}^H T)/M$ and $([2(k-1)\pi + \omega_s{}^H T])/M$ respectively. The passband and stopband edge of the masking filter $F_1(z)$ is $(2k\pi + \omega_c{}^H T)/M$ and $(2k\pi - \omega_s{}^H T)/M$ respectively. M is determined form step 1 and k = $\left\lceil \frac{M\omega_s T}{2\pi} \right\rceil$.
5) Designing the model filter and masking filter with 50% ripple margin approximately.
6) Verifying the frequency response of the resulting FRM filter. If specification is not met then increase the ripple margin slightly and go to step 3 and step 4 [22].

Design example 5.1: Designing FIR low pass filter with following specification

$\omega_c T$(passband edge)=0.4π rad,

$\omega_S T$(stopband edge)=0.402π rad ,

δ_C(passband ripple)= 0.01 and

δ_s(stopband ripple) = 0.001

In this design we get from equation 5.14 with subfilter being optimized separetely [22]

$$M = \frac{1}{\sqrt{\frac{2*1}{\pi}(0.002\pi)}} = 15.811$$

Choosing M= 16 ,

Filter length (N) estimation :

In regards to estimation of filter length for a linear-phase lowpass filter following equation has been applied [22]:

$$N \approx \frac{D_\infty(\delta_c,\delta_s) - F(\delta_c,\delta_s)\left(\frac{\Delta\omega T}{2\pi}\right)^2}{\left(\frac{\Delta\omega T}{2\pi}\right)} \tag{5.17}$$

where

$$D_\infty(\delta_c,\delta_s) = [a_1(\log(\delta_c))^2 + a_2(\log(\delta_c) + a_3](\log(\delta_s) + a_4(\log(\delta_c))^2 + a_5(\log(\delta_c) + a_6$$

$$F(\delta_c,\delta_s) = b_1 + b_2(\log(\delta_c) - \log(\delta_s))$$

and $\Delta\omega T = \omega_s T - \omega_c T$

The constants are a_1=0.0005309, a_2=0.07114, a_3=-0.4761, a_4=-0.00266, a_5=-0.5941, a_6=-0.4278, b_1=11.01217, b_2=0.51255

Above equation for filter length estimation has been derived by Herrmann[30][31]. Parks, MaClellan and Rabinar [32] algorithm have been used in desinging of model filter H(z) and masking filters {$F_0(z)$ and $F_1(z)$}.Using the equation 5.17, for design specification mentioned in example 5.1, filter length of the model filter H(z) is 164 while filter length of masking filters $F_0(z)$ and $F_1(z)$ is 82 and 88 respectively.The filter length of overall filter H(z) is 1730.

Magnitude response of filters:-

Magnitude response of periodic model filter and masking filters(shown together in dB).

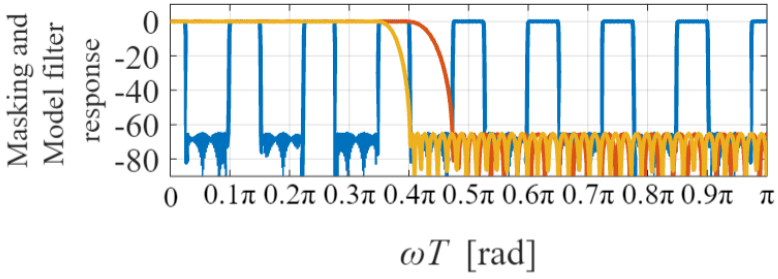

Figure 71 Magnitude response of masking and periodic model filters. [Periodic model filter shown with blue color. Red and yellow color indicates masking filter $F_0(z)$ and $F_1(z)$ respectively.]

Magnitude response of two branches for FRM :

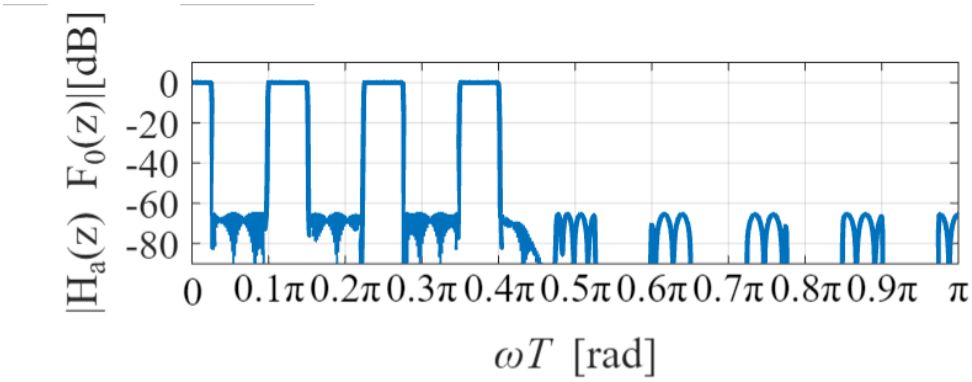

Figure 72 Magnitude response of upper branch ($|H_a(z).F_0(z)|$).

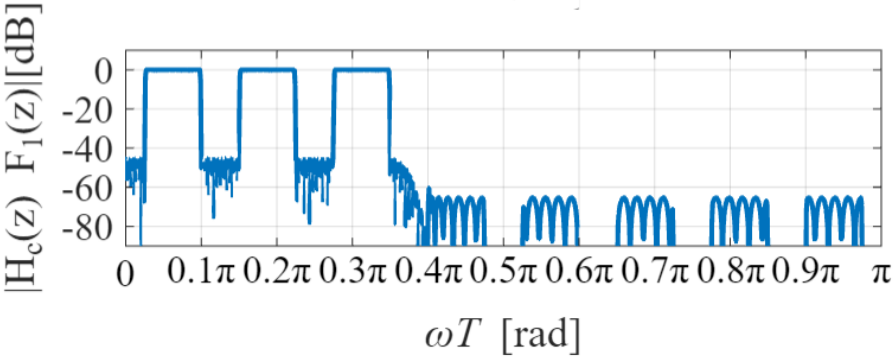

Figure 73 Magnitude response of lower branch ($|H_c(z).F_1(z)|$) .

Magnitude response of the overall filter :

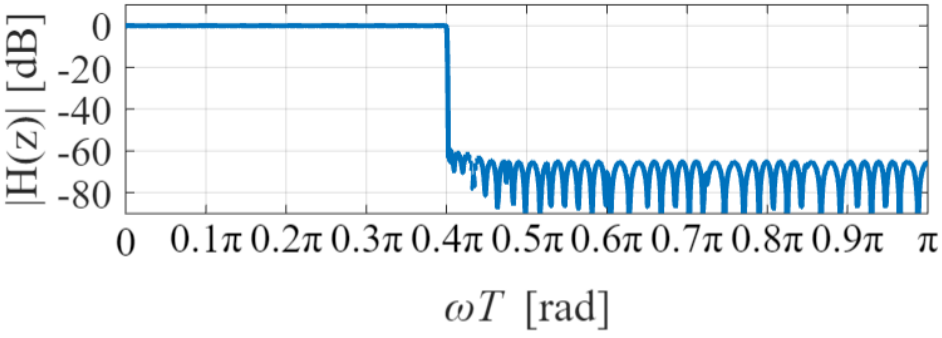

Figure 74 Magnitude response of overall filter.

Window method	Approximate filter length(N)	Minimum stopband attenuation (in dB)
Rectangular	2000	56.47
Von Hann	4000	48.23
Hamming	4000	52.79
Bartlett	4000	60.79
Blackman	6000	62.58
Kaiser	3500	57.27
FRM Method	**Approximate filter length(N)**	**Minimum stopband attenuation (in dB)**
Frequency Masking technique	1730	64.91

Table 6 Approximate filter length (N) and stopband attenuation (A_s) comparison with window method for design example 5.1.

Results

Order of overall filter for design example explained in this chapter is 1730 which is much less than the order required for same design specifications of FIR filter using window technique. Table 6 shows the filter length and stop band attenuation for same specification when designed with window technique. The FRM technique has better stop band attenuation and lower filter length as compare to the window method. This reduction in the filter length (N) leads to lower number of multiplication and additions required along with less computation time.

5.6 Summary

In this chapter the design of narrow band FIR filters using two up sampling and two masking filters has been discussed. It is shown that this approach allows for better control of the final filter's bandwidth than the method of chapter 4. The role of the complementary pair and masking filters is presented along with a design example of FIR filter. Even though the window method is quite easier to apply and design compared to frequency masking technique, it suffers from large filter length resulting in a greater number of additions and multiplications. Larger number of addition and multiplication leads to more computations. The frequency masking technique provides better selectivity over the window method for designing narrowband low pass filters.

Chapter 6

6.1 Conclusion

The designing of FIR filters illustrated in this project provides an overview of efficiency of frequency masking technique over the conventional window FIR filter design method. Performance comparison of both techniques were shown using design examples. In the introduction of this report the motivation for choosing this project and different methods of designing FIR filters have been discussed. The concept of frequency masking technique was introduced.

In chapter 2 and 3, filter specifications needed to design FIR filter were discussed in detail, along with different types of FIR filters. The Gibbs's phenomena and their impact on filter design was discussed. Using different window functions, FIR filters were designed and the stopband attenuation was evaluated. The order of narrow band low pass filter was evaluated for performance comparison with frequency masking technique.

In Chapter 4, narrow band lowpass FIR filters were designed using one FRM filter but they lacked the flexibility to control the bandwidth. A design example using FRM involving one masking filter illustrated that the order required for narrow band low pass FIR filters is less compared to window technique with the same specifications.

In Chapter 5, the challenge of control on bandwidth was resolved using a technique when FRM uses two making filters instead of one. The role of complementary pair and masking filters was discussed. A design example showed that the order required is less in case of FRM technique over the window method.

6.2 Future work

Frequency-response masking techniques has successfully been extended to many other filter categories, such as approximately power complementary filter pairs [33], half band filters [34], Hilbert transformers [35], interpolation and decimation filters [36], two channel filter banks (FBs) [37], modulated trans multiplexers [2], and two dimensional filters [26].

Recent advancements in optimization techniques, has been subject of interest. Convex-concave procedure (CCP) and other optimization technique have led to design techniques for further reduction in complexity. Application of CCP in multistage FRM filter design is very promising, and seems worthwhile for consideration as topic for future research.

Bibliography

[1] Y. C. Lim, “Frequency-response masking approach for the synthesis of sharp linear phase digital filters,” IEEE trans. circuits syst., vol. 33, pp. 357–364, Apr. 1986.

[2] Y. C. Lim and Y. Lian, “The optimum design of one- and two-dimensional FIR filters using the frequency response masking technique,” IEEE trans. circuits syst. II, vol. 40, pp. 88–95, Feb. 1993.

[3] J. F. Kaiser, “Non recursive digital filter design using *i*0-sinh window function,” in Proc.

IEEE Int. Symp. circuits syst., Apr. 1974, pp. 20–30.

[4] Lim, Y.C., Lian, Y.: Frequency-response masking approach for digital filter design: complexity reduction via masking filter factorization. IEEE trans. circuits syst. part II 41, 518–525 (1994).

[5] J.W Adams and A.N Willson, Jr., Some efficient digital prefilter structures, IEEE trans. circuits syst., vol. CAS-31, pp. 260-265, Mar. 1984.

[6] G. Hill, “The benefits of under sampling,” Electronic design, July 11, 1994.

[7] Introduction to digital signal processing using MATLAB with application to digital communications, K.S Thyagarajan.

[8] Streamlining digital signal processing, second edition 2012.

[9] Window functions and their applications in signal processing, K.M.M Prabhu.

[10] Design of narrow transition band variable bandwidth digital filter, Subhabrata Roy and Abhihit Chandra. ISSN 1751-858X.

[11] J.W Adams and A.N Willson, Jr., A new approach to FIR digital filters with fewer multipliers and reduced sensitivity, IEEE trans. circuits sys., vol. CAS-30, pp 277-283, May. 1983.

[12] M.G Bellanger, Improved design of long FIR filters using the frequency masking technique, IEEE Int. conf. acoust., Speech signal processing, 1996, pp. 1272-1275.

[13] Z Jing and A.T. Fam, A new structure for narrow transition band lowpass digital filter design, IEEE trans. acoust., Speech, signal processing, vol. ASSP-32, pp. 362-370, Apr. 1984.

[14] Design of sharp linear phase FIR band stop filters using the frequency response masking technique by Rui Yang, Yong-Ching Lim and Sydney R. Parker. Circuit system signal processing vol 17, no.1,1998, pp. 1-27.

[15] Wanhammar, L., Yu, Y.J.: Digital filter structures and their implementation. In: Academic Press Library in Signal Processing: Signal processing theory and machine learning, vol. 1, Chapter 6 (2013).

[16] T. Saramaki. "Design of computationally efficient FIR filters using periodic sub filters as building blocks," in Circuits and filters handbook. edited by W.-K. Chen, CRC Press, pp. 2578-2601, 1995.

[17] T. Saramaki and Y. C. Lim. "Use of the Remez algorithm for designing FIR filters utilizing the frequency response masking approach," in Proc. IEEE 7th. symp. circuits syst., pp. 449-455, Orlando, FL. May 1999.

[18] H. Johansson, T. Saramaki and J. Yli-Kaakinen, “Optimization of frequency response masking based FIR Filters”, J. Circuits, Systems, and computers, vol. 12, no. 5, pp. 563–591, 2003.

[19] S. R. K. Dutta and M. Vidyasagar, “New algorithms for constrained minimax optimization,” Math. programming, vol. 13, pp. 140–155, 1977.

[20] L. R. Rabiner and B. Gold, Theory and Application of Digital Signal Processing. Prentice-Hall, 1975

[21] A. V. Oppenheim and R. W. Schafer, Digital Signal Processing. Prentice-Hall, 1975. (Chapters 4-5).

[22] Lar Wanhammar and Tapio Saramaki, Digital filters using MATLAB.

[23] Multirate Filtering for digital signal processing: MATLAB Application.

[24] Digital signal processing, Principle, algorithms and application fourth edition by John G Proakis and Dimitris G. Manolakis.

[25] Digital Filters: Principles and Applications with MATLAB, First Edition. Fred J. Taylor. © 2012 by the Institute of Electrical and Electronics Engineers, Inc. published 2012 by John Wiley & Sons, Inc.

[26] Interpolated Finite impulse response filters, Yrjo Neuvo, Dong Cheng-yu and Sanjit K Mitra. IEEE transactions on acoustics, speech, and signal processing, vol. ASSP-32, no. 3, June 1984.

[27] Signals, processes, and systems, an interactive multimedia introduction to signal processing, third edition by Ulrich Karrenberg.

[28] Digital signal processing, signal system and filter, Andreas Antoniou.

[29] Lim, Y.C., Yang, R.: On the synthesis of very sharp decimators and interpolators using the frequency-response masking technique. IEEE Trans. Signal Process. 53(4), 1387–1397 (2005)

[30] Herrmann, O., Rabiner, R.L., Chan, D.S.K.: Practical design rules for optimum finite impulse response digital filters. Bell Tech. J. 52(6), 769–799 (1973).

[31] Rabiner, L.R., Gold, B.: Theory and application of digital Signal processing. Prentice Hall, Englewood Cliffs, N.J. (1975).

[32] McClellan, J.H., Parks, T.W., Rabiner, L.R.: A computer program for designing optimum FIR linear phase digital filters. IEEE trans audio electro acoust. 21(6), 506–526 (1973).

[33] Saramäki, T., Lim, Y.C., Yang, R.: The synthesis of half-band filter using frequency-response masking technique. IEEE Trans. circuits syst. part II 42(1), 58–60 (1995).

[34] T.Deng, "Low complexity design of 2-D half band filters," 2009 9th International symposium on communication and information technology, 2009, pp. 602-604, doi:10.1109/ISCIT.2009.5341176.

[35] Milić, L., Certic, J.D., Lutovac, M.: A class of FRM-based all-pass digital filters with applications in half band filters and Hilbert transformers. In: ICGCS Conference on green circuits and systems (2010).

[36] Johansson, H., Saramäki, T.: Two channel FIR filter banks utilizing the frequency response masking approach. Circuits syst. signal process. 22(2), 157–192 (2003)

[37] Diniz, P.S.R., de Barcellos, L.C.R., Netto, S.L.: Design of high resolution cosine modulated transmultiplexers with sharp transition band. IEEE trans. signal process. 52(5), 1278–1288 (2004)